

Review

# Review of Electric Vehicle Converter Configurations, Control Schemes and Optimizations: Challenges and Suggestions

Molla S. Hossain Lipu <sup>1,\*</sup>, Mohammad Faisal <sup>2</sup>, Shaheer Ansari <sup>1</sup>, Mahammad A. Hannan <sup>3</sup>, Tahia F. Karim <sup>4</sup>, Afida Ayob <sup>1</sup>, Aini Hussain <sup>1</sup>, Md. Szal Miah <sup>5</sup> and Mohamad Hanif Md Saad <sup>6</sup>

<sup>1</sup> Department of Electrical, Electronic and Systems Engineering, Universiti Kebangsaan Malaysia, Bangi 43600, Malaysia; p100855@siswa.ukm.edu.my (S.A.); afida.ayob@ukm.edu.my (A.A.); draini@ukm.edu.my (A.H.)

<sup>2</sup> Department of Electrical and Electronic Engineering, International Islamic University Chittagong, Chattogram 4318, Bangladesh; mfaisal@iiuc.ac.bd

<sup>3</sup> Department of Electrical Power Engineering, College of Engineering, Universiti Tenaga Nasional, Kajang 43000, Malaysia; hannan@uniten.edu.my

<sup>4</sup> Department of Electrical and Electronic Engineering, American International University-Bangladesh, Dhaka 1229, Bangladesh; tahia.karim@aiub.edu

<sup>5</sup> School of Engineering and Technology, Asian Institute of Technology, Pathumthani 12120, Thailand; st121577@ait.asia

<sup>6</sup> Institute of IR 4.0, Universiti Kebangsaan Malaysia, Bangi 43600, Malaysia; hanifsaad@ukm.edu.my

\* Correspondence: lipu@ukm.edu.my

**Abstract:** Electric vehicles are receiving widespread attention around the world due to their improved performance and zero carbon emissions. The effectiveness of electric vehicles depends on proper interfacing between energy storage systems and power electronics converters. However, the power delivered by energy storage systems illustrates unstable, unregulated and substantial voltage drops. To overcome these limitations, electric vehicle converters, controllers and modulation schemes are necessary to achieve a secured and reliable power transfer from energy storage systems to the electric motor. Nonetheless, electric vehicle converters and controllers have shortcomings including a large number of components, high current stress, high switching loss, slow dynamic response and computational complexity. Therefore, this review presents a detailed investigation of different electric vehicle converters highlighting topology, features, components, operation, strengths and weaknesses. Moreover, this review explores the various types of electric vehicle converter controllers and modulation techniques concerning functional capabilities, operation, benefits and drawbacks. Besides, the significance of optimization algorithms in electric vehicle converters is illustrated along with their objective functions, executions and various factors. Furthermore, this review explores the key issues and challenges of electric vehicle converters, controllers and optimizations to identify future research gaps. Finally, important and specific suggestions are delivered toward the development of an efficient converter for future sustainable electric vehicle applications.

**Keywords:** DC-DC converter; electric vehicle; intelligent controller; modulation techniques; meta-heuristic optimization; battery storage systems



check for updates

**Citation:** Lipu, M.S.H.; Faisal, M.; Ansari, S.; Hannan, M.A.; Karim, T.F.; Ayob, A.; Hussain, A.; Miah, M.S.; Saad, M.H.M. Review of Electric Vehicle Converter Configurations, Control Schemes and Optimizations: Challenges and Suggestions. *Electronics* **2021**, *10*, 477. <https://doi.org/10.3390/electronics10040477>

Academic Editor: Bor-Ren Lin  
Received: 28 December 2020  
Accepted: 19 January 2021  
Published: 17 February 2021

**Publisher's Note:** MDPI stays neutral with regard to jurisdictional claims in published maps and institutional affiliations.



**Copyright:** © 2021 by the authors. Licensee MDPI, Basel, Switzerland. This article is an open access article distributed under the terms and conditions of the Creative Commons Attribution (CC BY) license (<https://creativecommons.org/licenses/by/4.0/>).

## 1. Introduction

The world climate and environment are facing serious threats due to the carbon emission caused by diesel-based vehicles [1,2]. The increased use of fossil fuels in diesel-based vehicles is one of the main reasons for global warming and climate change issues [3,4]. A recent report suggests that transportation is responsible for contributing 24% of global carbon emissions [5]. Another study by the European Union mentions that carbon dioxide (CO<sub>2</sub>) emissions by the transport sector are approximately 27%, while 70% of emissions are directly emitted by vehicle transport [6]. To address these concerns, electric vehicles (EVs) have received massive attention around the world due to their zero carbon emissions, low noise, light weight, improved performance and efficiency [7,8]. However, EVs are facing

challenges with regard to battery cost, recharge time and driving range [9,10], as well as the proper functionality of various types of converters in the EV drivetrain [11,12]. The efficient functionality of EVs requires appropriate interfacing between energy storage systems (ESSs) and power converters as well as advanced driver assistance systems, acceleration slip regulation, active control systems and anti-lock brake systems. Ding et al. [13] evaluated the longitudinal vehicle speed of EVs using multi-sensor fusion with a low-cost inertial measurement unit, BeiDou navigation positioning module and global positioning system. Zhang et al. [14] developed a robust sliding mode controller for motor-driven EVs to obtain a robust and accurate motion control of EVs. A time delay objective function with a linear quadratic regulator problem is formulated to decrease the control efforts and tracking error. The simulation and hardware-in-the-loop (HIL) tests confirmed that the proposed controller enhanced the lateral stability of the vehicle in comparison to another optimal controller scheme.

EVs are structured using different types of ESSs connected with various types of power electronic converters [15–17]. Generally, ESSs are charged by taking current and voltage from the grid or charging stations through AC-DC converters [18]. Afterwards, ESSs deliver the required energy to the motor to accelerate the vehicle. However, the power delivered by ESSs has unstable characteristics and considerable voltage drops [19–21]. Thus, DC-DC converters play a key role in converting the unregulated power flow to a regulated one [22–24]. Zhang et al. [25] presented the research progress of hybrid ESS development focusing on sizing, DC/DC converter configuration and an energy management strategy in EV applications. The effectiveness of the proposed topology was verified using a case study and the results indicated a reduction of the battery degradation rate by 40% in comparison to the battery-based storage system. Nonetheless, the appropriate design of DC-DC converters is challenging since it depends on input voltage, duty cycle and load parameters [26–28]. In addition, DC-DC converters present non-linear behavior and lightly damped dynamics due to the switching actions [29,30]. To overcome the non-linearity issues, as well as achieve fast dynamics and desired output voltage, the design of an efficient controller is an urgent necessity.

The main purpose of using a controller in EV converters is to obtain steady-state and dynamic characteristics with short settling time, a faster response and few steady-state errors [31,32]. A quick dynamic response reduces electromagnetic interference (EMI), switching losses and current stress. Various types of linear and non-linear controllers are being employed to control the DC-DC converters in EVs [33]. Linear controllers have a simple construction and easy implementation; however, they are ineffective under parameter variation and load disturbance [34,35]. To address these shortcomings, intelligent controllers are utilized and have been successful in achieving excellent dynamics, improved stability and outstanding transient response [36,37]. In addition, intelligent controllers have a robust, flexible and smooth execution and can handle highly non-linear and complex systems with imprecise inputs [38–40].

The optimization algorithm in EV converters aims to optimize the design as well as to meet various performance requirements while many constraints are taken into consideration [41,42]. The design of the converter can be upgraded by reducing the number of passive components, weight and associated cost. In line with that, the effectiveness of the converter can be improved by reducing converter loss, switching angle and input current ripple [43]. A multi-objective function helps to achieve all the necessities toward the development of an advanced converter in EVs [44]. However, the formulation of a multi-objective function is a laborious task and lots of parameters, variables and constraints need to be assigned, including input current, weight, number of phases and switching frequency.

A few notable review articles have addressed converter design and operation in EVs. Chakraborty et al. [45] explored various DC-DC converters in EVs, focusing on converter topologies and evaluation criteria. Nevertheless, they did not explain the controller and optimization methods and related implementation issues of various converters in EVs.

Jagadeesh and Indragandhi [46] outlined and compared different DC-DC converters in EV applications. However, the explanation of the converter was limited to only a few methods. Moreover, the operation, control and optimization of the converter were not studied in detail. Bellur et al. [47] overviewed the DC-DC converters in vehicular applications. Nonetheless, the authors did not highlight the key implementation issues explicitly. Anbazhagan et al. [48] presented bidirectional DC-DC converters for EV applications, highlighting both isolated and non-isolated converters; however, the operation, control, modulation and optimization were not discussed in detail. Krithika and Subramani [49] reviewed various power converters in hybrid electric vehicles (HEVs) concerning unidirectional, bidirectional, isolated and non-isolated types. Nonetheless, the authors did not provide a detailed explanation of each converter. Moreover, the intelligent control schemes and modulation techniques of the converters were not covered in detail. Kumar et al. [50] focused on power conversion topologies, highlighting various viable converters and controllers in HEV applications. However, the authors did not provide the categorization of the converters and implementation issues.

To bridge the existing research gaps, this review unveils new contributions with a detailed investigation of converters in EVs. The review offers the following contributions:

- A comprehensive explanation of various DC-DC converters for EVs is delivered. In line with that, the classification of EV converters along with their structure, execution process, purpose, achievements, benefits and drawbacks are provided.
- The categories of EV converter controllers, including linear controllers and intelligent controllers, are reported. Besides, the various functional features, control operation, target, contributions, merits and demerits are discussed thoroughly.
- The modulation schemes employed in various controllers in EVs are outlined concerning the target and outcomes.
- The EV converter optimization algorithms with respect to objective functions, constraints, pros and cons are highlighted.
- The existing issues and challenges of EV converters, controllers, modulation and optimization approaches with regard to design, implementation, computational complexity, objective function and performance are explained rigorously.
- Selective future proposals for the design and progress of an efficient converter are delivered.

Content analysis was chosen to conduct this survey. The appropriate article selection of this review was carried out through three screening phases. The first screening was the literature survey which was performed using the Google Scholar, Scopus science database, Web of Science and Research Gate platforms. A total of 638 articles were explored after the first screening. Next, the second screening was carried out using important keywords, including DC-DC converter, electric vehicle, intelligent controller, modulation techniques, metaheuristic optimization, battery storage systems. Apart from keywords, the paper title, abstract and article contents were viewed to find the relevant articles. The authors identified a total of 372 articles after the second screening. Afterward, the third screening and assessment were conducted based on the number of citations, review process and impact factor and, accordingly, a total of 180 articles published in recent conference proceedings, books, recognized webpages and notable journals were identified. The authors read the selected 180 articles thoroughly to extract useful information as well as carry out critical review, analysis and discussion relating to EV converters, controllers, modulation, optimization, issues and challenges. The schematic diagram of the reviewing methodology is shown in Figure 1.

The results obtained through the three screening phases were divided into five groups. Firstly, EV converter classification, topologies, operation, contributions, strengths and weaknesses are provided. Secondly, EV converter controller types, characteristics, control operation, targets, contributions, benefits and shortcomings are discussed. Besides, EV converter modulation schemes were explored. Thirdly, EV converter optimization algorithms along with their objective functions, constraints, advantages and disadvantages are highlighted. Fourthly, numerous key issues and challenges of EV converters and related

controllers and optimization were identified. Lastly, the review offers some important proposals for future improvements of EV converters toward sustainable EV development.

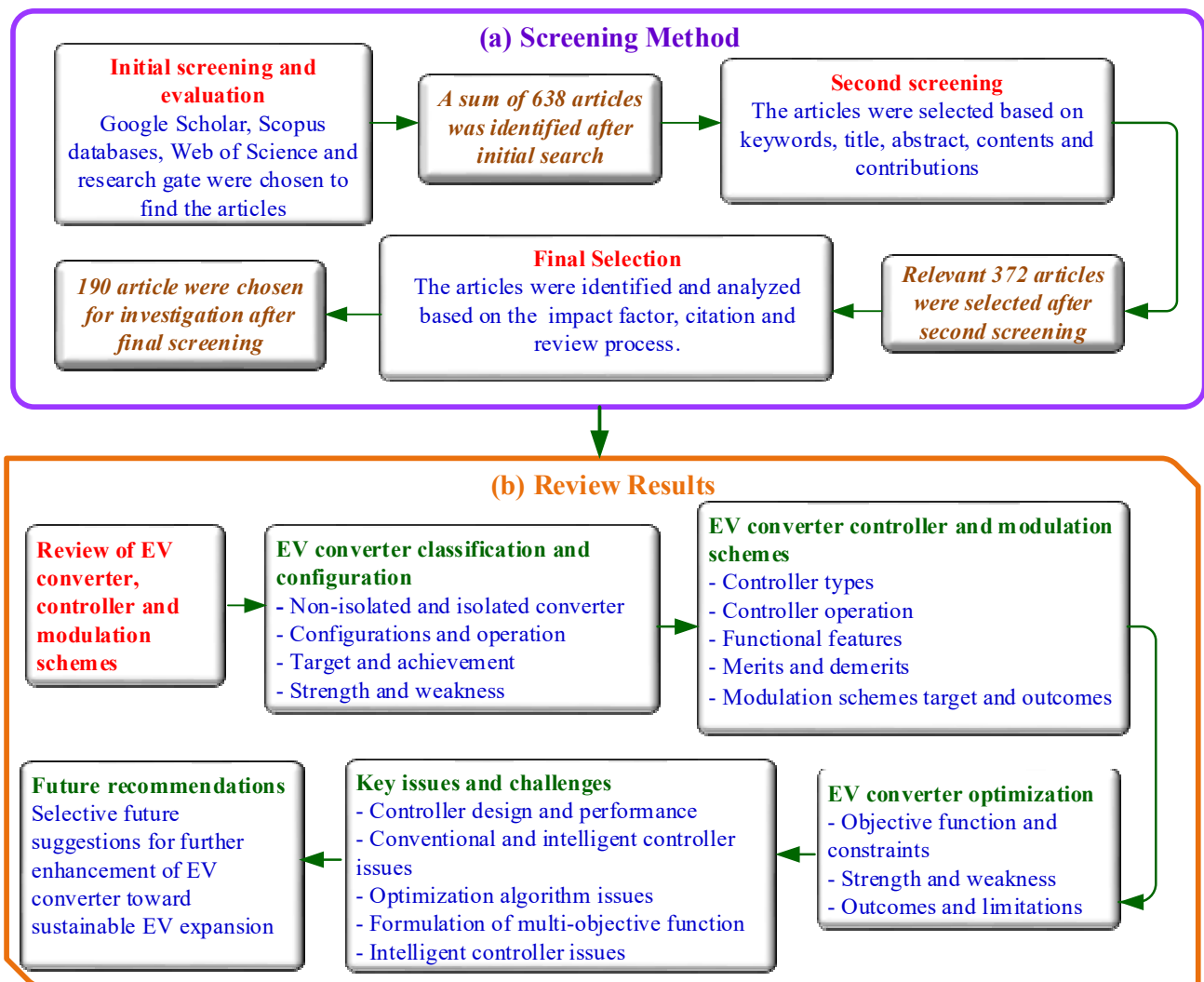


**Figure 1.** Schematic diagram of the reviewing methodology. EV: electric vehicle.

The paper is structured into seven sections. Section 2 gives the overview of EV converters under control, modulation and optimization strategies. Section 3 covers the detailed classification and explanation of various DC-DC converters in EVs. The EV converter controller types, characteristics and operation are explained in Section 4. In line with that, this section also discusses the EV converter modulation schemes. The role of optimization algorithms in EV converters is covered in Section 5. The current issues and research gaps are highlighted in Section 6. The concluding comments and future recommendations are outlined in Section 7.

## 2. Overview of EV Converter Controllers, Modulations and Optimizations

The architecture of an EV drivetrain includes ESSs, converters, controllers, modulation, optimization and an electric motor. ESSs, including a battery, supercapacitors (SCs) and fuel cells (FCs), are connected to a DC-DC converter through a suitable controller and modulation scheme. The connection from the DC-DC converter to the electric motor is established through a high-voltage (HV) DC bus follows by a DC-AC inverter, as presented in Figure 2.

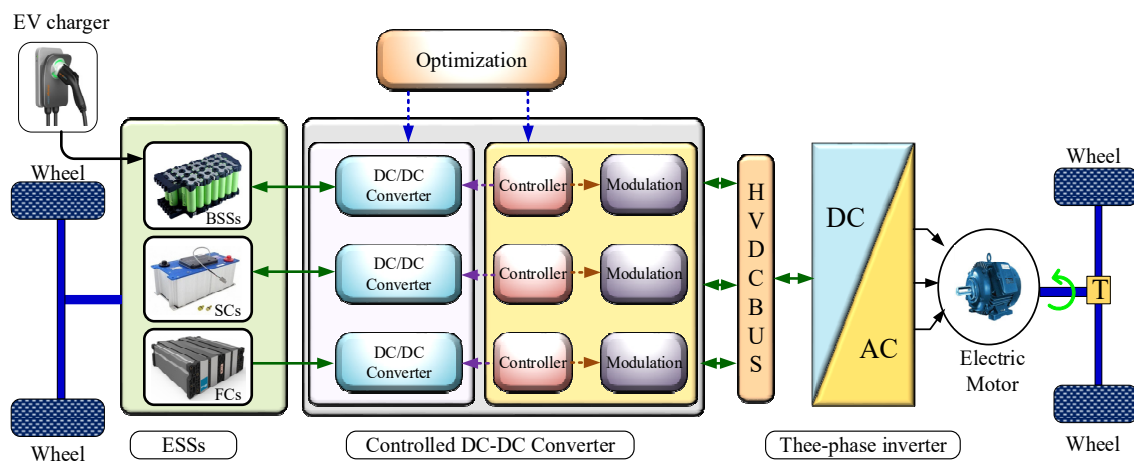


**Figure 2.** The layout of EV drivetrain with converters under suitable control, modulation and optimization integrated with various ESSs. EV: electric vehicle; BSSs: battery storage systems; SCs: supercapacitors; FCs: fuel cells; HV: high voltage; T: Transmission

ESSs are responsible for delivering stable and consistent power to the motor; however, they suffer from unregulated behavior, voltage drops and slow dynamic responses. The battery storage system (BSS) exhibits compact size, high energy density and mature reliability and hence is suitable to provide a lifelong energy supply [51]. The SCs offer low energy density but they have fast charging and discharging capabilities which make them ideal for delivering power instantaneously at high acceleration [52]. Thus, the hybrid energy storage system combining BSSs and SCs can bring benefits in terms of long lifecycle, fast response and low stress to the batteries; however, the cost of the entire storage system increases [53]. In the case of FCs, they provide high energy density but have shortcomings including high cost, slow dynamic response and limited supporting infrastructure.

To connect the ESS with the HV DC link of the drivetrain, each DC-DC converter needs definite requirements and specifications. Firstly, bidirectional DC-DC converters support regenerative braking and improve efficiency [54–56]. Secondly, a DC-DC converter with appropriate control and modulation is necessary to carry out fast charging and discharging operations in SCs as well as to avoid incompatible operations [57–59]. Thirdly, the topology of a DC-DC converter with few passive components is preferred for SCs to minimize the transition duration between the charging and discharging phases [60–62]. On the contrary, fast dynamic control is not required in the case of BSSs due to long interval charging profiles [63]; however, the lower input current ripples are suitable to extend the lifespan of BSSs [64,65]. Fourthly, a DC-DC converter in EVs exhibits a high voltage gain and high power output [66–68]. Fifthly, BSSs and SCs obtain low output voltage; hence, an HV DC-DC converter is needed to achieve a high voltage level by storing the energy either in capacitors or inductors using diodes, insulated gate bipolar transistors (IGBTs) and metal–oxide–semiconductor field-effect transistors (MOSFETs) [28,69–71]. An ideal DC-DC converter offers several benefits, including low price, light weight, compact size, efficiency, scalability and controllability, which are highly desirable in the EV automotive industry [72–74]. Regardless of having many benefits, an HV DC-DC has several shortcomings, such as low efficiency because of hard-switching, very flat voltage gain, incapability to achieve high power density and difficulties to construct a high bandwidth control loop [75–79].

The various controllers and modulation are integrated with the converter to elevate the performance and robustness. An efficient controller is important to attain proper coordination and management of ESSs, fast tracking, reliable power distribution and lower steady-state error [80–82]. Besides, the modulation technique is crucial to achieve a controlled output voltage/current, low harmonics and low switching losses. To enhance the control operational efficiency of the converter, optimization algorithms can be employed.

The aim of the optimization in a converter is to achieve a low ripple current and reduce converter loss, the number of components and development time [43,83–85].

### 3. EV Converter Types and Configurations

The complete classification of EV converters, including topology, control, modulation and optimization, is presented in Figure 3. The configuration of converters in EVs can be categorized into two groups: non-isolated and isolated. The non-isolated converter is appropriate for EVs under medium- and high-power operation [86,87], while isolated DC-DC converters are suitable in EVs with low- and medium-power purposes [88,89].

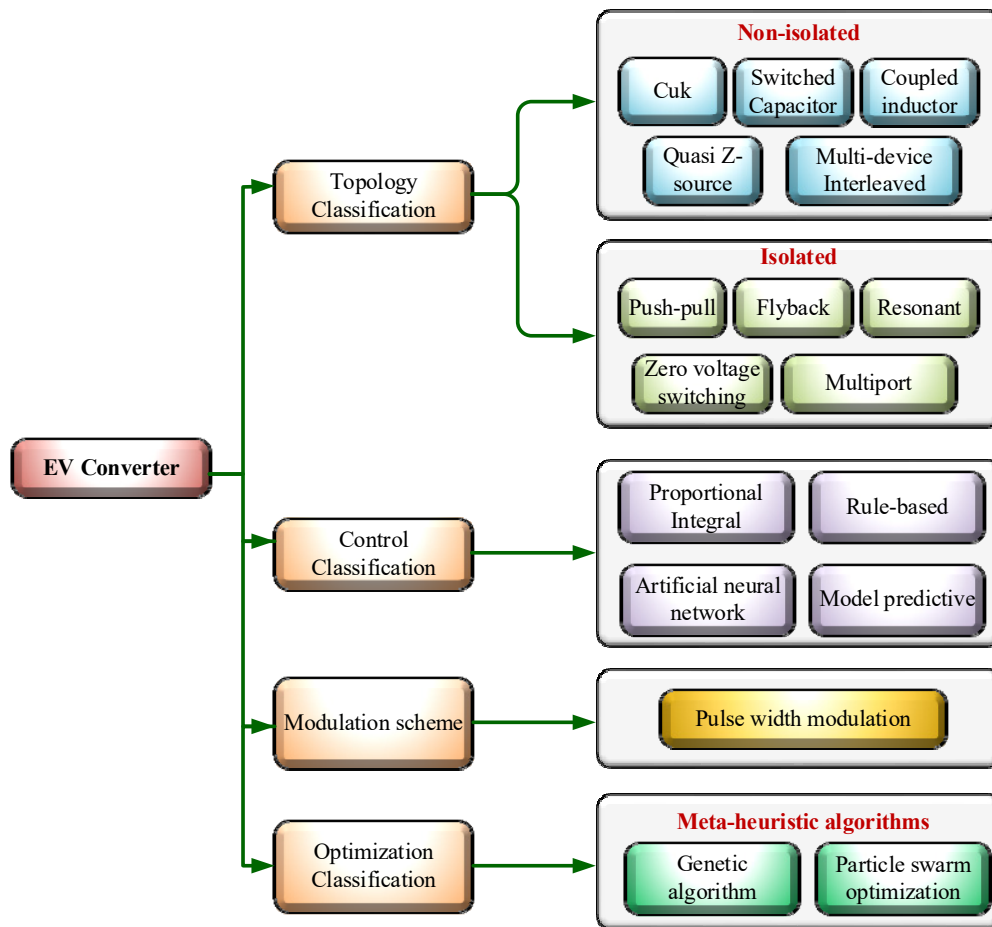


**Figure 3.** The comprehensive classification of EV converters, including configuration, control, modulation and optimization. EV: electric vehicle.

#### 3.1. Non-Isolated Converter

Non-isolated bidirectional DC-DC converters includes conventional DC-DC converters and interleaved DC-DC converters. Among them, conventional DC-DC converters are commonly employed due to their low cost, simple topology and easy control technique. The interleaved DC-DC converters have become popular due to their improved performance and efficiency.

##### 3.1.1. Cuk Converter

The Cuk converter (CC) in EVs provides flexibility to regulate the output to be lower or higher in comparison to the input voltage. The CC features a lower output ripple and improved efficiency since it shares a single magnetic core [63]. Besides, the CC has uniformity of the current at both the input and output terminal as well as continuous power transfer through the capacitor, leading to lower EMI radiation in the switches. Additionally,

the CC implements an L-C filter which can regulate the peak-to-peak ripple current of the inductor more efficiently than a DC-DC buck–boost converter. However, the CC suffers from some losses due to high current stress on the switch and the larger number of reactive components [90].

Pandey and Singh [91] designed a converter with an improved power factor for EV charging by utilizing a DC-DC CC. The power factor was corrected through the continuous conduction mode of the primary inductor operated by the CC. The design was modeled and simulated in MATLAB. Ananthapadmanabha et al. [63] presented an improved CC for EV battery charging applications by utilizing a switched inductor. The author discussed several aspects, like modeling, analysis, simulation and experimentation results. The proposed converter was rated at 500 W, 48 V/10.4 A. The performance of the converter was evaluated based on total harmonic distortion (THD). Reshma et al. [92] designed a proportional integral (PI) controller-based CC to operate the electric motor in vehicular applications under two operational modes: accelerate and regenerative. In addition, four-quadrant operation was implemented by the authors to validate the effectiveness of the CC. The reports illustrated that the CC delivered stable and ripple-free output in comparison to the parallel switch boost converter.

The CC topology for EV applications is designed using two inductors, two capacitors and two switches, as shown in Figure 4a. The capacitor transfers energy alternately through the commutation between switches. Besides, inductors  $L_1$  and  $L_2$  help to transform the energy from the BSS to the electric motor. Moreover, the CC can operate in both continuous and discontinuous current mode operation. The output voltage  $V_o$  across the load during the continuous mode of operation for the DC-DC CC is expressed as [92]

$$V_o = V_i \left( \frac{-D}{1-D} \right) \quad (1)$$

where  $V_i$  and  $D$  stand for the input voltage and duty cycle, respectively.

### 3.1.2. Switched-Capacitor Bidirectional Converter

The switched-capacitor bidirectional converter (SCBC) in EVs utilizes synchronous rectification to execute the turn-on and turn-off operations. The SCBC does not require extra components and has improved power conversion efficiency through the proper utilization of power switches [93–95]. However, the SCBC has low voltage stress, a wide-reaching voltage gain and needs a smaller number of components. Besides, the SCBC suffers from a high ripple current and cannot offer high efficiency under widespread input to output voltages.

Zhang et al. [96] designed an SCBC for an EV application without the magnetic coupling that can deliver continuous inductor current and a stable switched-capacitor voltage through the switched capacitors. A prototype was developed with a capacity of 300 W with a high and low voltage of 300 V and 40~100 V, respectively. An efficiency of more than 90% was obtained under both step-up and step-down modes. Janabi and Wang [97] proposed a switched capacitor voltage boost converter for an EV application. The proposed topology replaced the traditional voltage source inverter (VSI) with a doubling of the area of the linear modulation region and eliminating both the large inductor in the boost DC-DC stage and the large filtering capacitor which thus resulted in higher energy density and a lower cost. Zhang et al. [98] developed a hybrid bidirectional DC-DC converter with an SCBC for hybrid energy source-based EVs. The proposed SCBC achieved lower voltage stress under wide-ranging voltage gain. The authors designed an experimental prototype of the converter rated at 400 W to verify the characteristic and theoretical analysis. Liu et al. [99] suggested an integrated voltage balancing topology for series-connected battery packs using a parallel-connected switched-capacitor (PCSC) converter and coupled buck–boost (CBB) converter. The proposed topology was validated using the two experimental prototypes applied to series-connected Li-ion battery strings. The results indicated that the CBB–PCSC equalizer performed better than other conventional

equalizers with regard to cost, size, efficiency and balancing speed. Shang et al. [100] proposed a compact high-frequency heater based on a resonant switched-capacitor (RSC) converter to obtain self-heating for lithium-ion batteries. The performance and theoretical analysis of the proposed configuration were verified using an experimental test bench with a temperature chamber, dSPACE, MOSFETs, power analyzer and six series-connected Li-ion batteries. The proposed topology illustrated excellent reliability, cost-effectiveness and achieved a good trade-off between high efficiency (96.4%) and fast heating speed (2.67 °C/min).

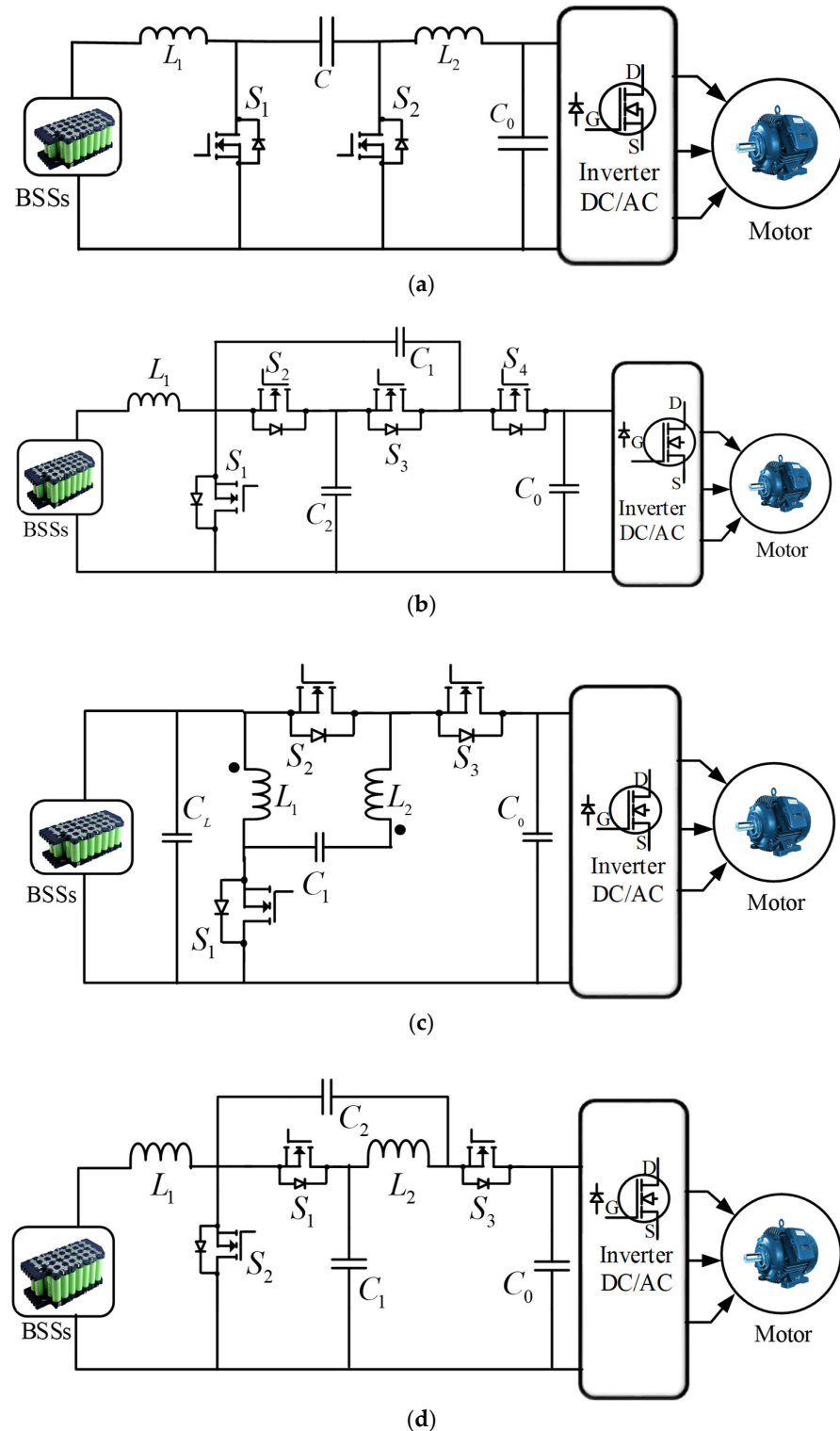
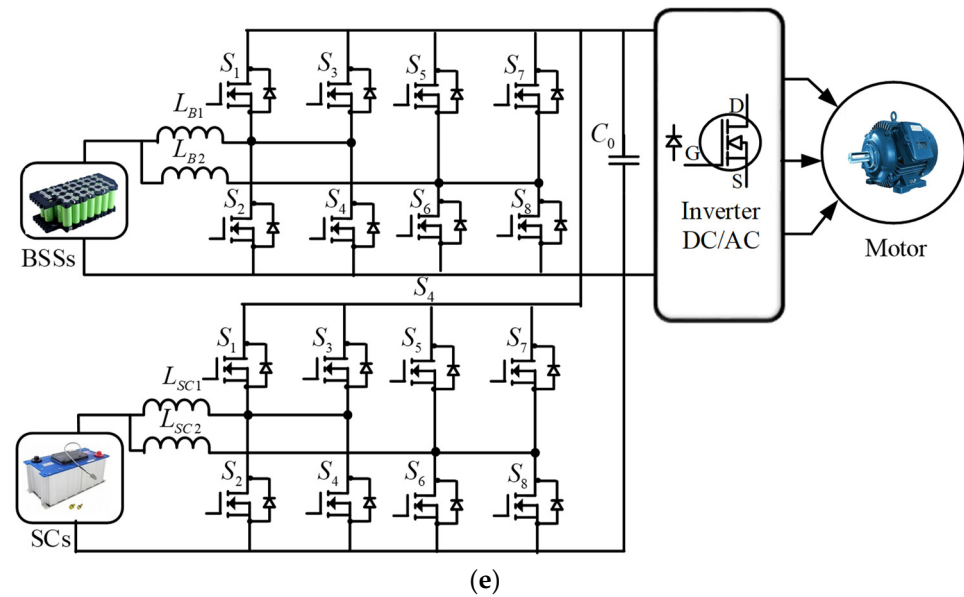


Figure 4. Cont.



**Figure 4.** Configuration of a non-isolated DC-DC converter for EVs: (a) Cuk converter, (b) switched-capacitor bidirectional converter, (c) couple inductor bidirectional converter, (d) quasi-Z-source converter and (e) multi-device interleaved bidirectional converter.

This converter is designed using three capacitors ( $C_1$ ,  $C_2$ ,  $C_3$ ) and one inductor ( $L$ ) and four switches ( $S_1$ ,  $S_2$ ,  $S_3$  and  $S_4$ ), as depicted in Figure 4b. When the SCBC is under step-up mode, the switch ON operation is executed by  $S_1$  and  $S_3$  while the switch OFF operation is performed by  $S_2$  and  $S_4$ . The current is transferred from the BSSs to  $L$  while  $C_1$  is charged by  $C_2$ . On the contrary, when the SCBC is under the step-down mode, the switch ON and switch OFF operations are carried out by  $S_2$ ,  $S_4$  and  $S_1$ ,  $S_3$ , respectively.  $L$  is charged by  $C_2$  whilst  $C_1$  takes charge current from  $C_0$ . The motor takes energy from  $L$ ,  $C_2$  and  $C_0$  [96]. The voltage gain of the SCBC can be written as:

$$\frac{V_o}{V_i} = \frac{2}{1-D} \quad (2)$$

### 3.1.3. Coupled Inductor Bidirectional Converter

A coupled inductor bidirectional converter (CIBC) in EVs provides high efficiency due to its high voltage gain and low voltage stress [101]. Besides, the CIBC has secondary leakage inductance which results in low reverse recovery of the output diode [102]. Due to the usage of the heavy inductor in a power boost converter, a CIBC is much preferred as compared with multiple discrete inductors as it provides less iron loss and low inductor current ripples [103]. Furthermore, the CIBC offers other benefits including voltage transformation, changing the impedance of a circuit and galvanic isolation. However, one of the limitations of couple inductor technology is the introduction of leakage inductance, causing resonance and voltage spikes [104].

Gonzalez-Castano et al. [105] presented a CIBC converter to control the DC voltage in EVs. The effectiveness of the CIBC was validated with the buck and boost mode of operation which showed satisfactory results. Kascak [106] designed a CIBC topology to execute the bidirectional current flow between the input sources and the three-phase inverter in EVs. Ayachit et al. [107] proposed a CIBC converter for EV charging applications with a low part count and a wide voltage conversion ratio. The proposed converter consists of a smaller number of components as compared with other traditional DC-DC converters in EVs. Various electrical parameters, such as current and voltage stresses and DC voltage and current transfer functions, were derived from the proposed design. Wu et al. [108] developed a CIBC for an EV application to enhance the voltage gain and decrease the

switching voltage stress. An experimental model of the converter rated as 1 kW, 40–60 V to 400 V was designed to validate its performance.

The CIBC allows the reduction of the overall volume in comparison with the multi-core solution of other topologies of the converter. The configuration of the CIBC for an EV application consists of the presence of only one magnetic core which allows a smaller volume as compared with other topologies, as shown in Figure 4c. The voltage gain of the CIBC can be expressed as:

$$\frac{V_o}{V_i} = \frac{2 + n - D}{1 - D} \quad (3)$$

#### 3.1.4. Quasi-Z-Source Bidirectional Converter

The quasi-Z-source bidirectional converter (QZBC) is employed in EVs due to its advantageous features, including simple topology, common ground and wide-ranging voltage gain. Generally, a conventional two-level QZBC is designed for EV operation [109–111]. Besides, this converter offers low voltage stress with reasonable static and dynamic performance. However, it has the drawbacks of discontinuous input current and capacitance of high voltage stress.

Zhang et al. [112] proposed a QZBC for hybrid energy sources in EVs. The authors developed a 300 W prototype indicating 40~120 V and 240 V on the low voltage side and the high voltage side, respectively. The experimental results indicated that the highest and lowest efficiencies of 96.44% and 88.17% were achieved, respectively, in step-up and step-down mode with decreasing input current and low losses. Devarajan and Sivaraman [113] presented a novel bidirectional QZBC for EV applications. A fixed switching frequency was achieved by applying the smoothing technique to the function of the sliding surface. In addition, a proportional–integral–derivative (PID) controller was utilized in handling errors in current and voltage across the capacitor. Hu et al. [114] designed a battery storage system based on QZBC topology in EVs. The work discussed the steady-state power distribution operation under different operating modes, such as traction mode, regenerative mode and recovery mode. Furthermore, the optimization of battery current stress and dynamic power regulation are executed using various controllers including time-domain controllers and frequency-domain controllers.

A switched-quasi-Z-source network is built using two inductors ( $L_1, L_2$ ), three capacitances ( $C_1, C_2, C_0$ ) and three power switches ( $S_1, S_2$  and  $S_3$ ), as displayed in Figure 4d. The bidirectional power flow in the low-voltage and high-voltage sides is executed through the step-up and step-down operation processes, respectively. During the step-up mode,  $S_1$  is switched ON, and  $S_2$  and  $S_3$  are switched OFF. The capacitance  $C_1$  is discharged and, accordingly, power is transmitted to  $C_2$  and  $L_2$  via  $S_1$ . Voltage gain can be expressed as:

$$M_{Boost} = \frac{1 + D_{Boost}}{1 - D_{Boost}} \quad (4)$$

where  $M$  and  $D$  denote the voltage gain and duty cycle, respectively. During the step-down mode,  $S_1$  is switched OFF and  $S_2, S_3$  are switched ON. The capacitance  $C_1$  is discharged via  $S_2$  and  $L_1, L_2$  and  $C_2$  are charged via  $S_3$ . Accordingly, voltage gain can be written as:

$$M_{Buck} = \frac{D_{Buck}}{2 - D_{Buck}} \quad (5)$$

#### 3.1.5. Multi-Device Interleaved Bidirectional Converter

The multi-device interleaved bidirectional converter (MDIBC) has become increasingly popular in EVs because of its advantageous features, including size, cost-effectiveness, high efficiency and lower ripples [115]. The MDIBC in EVs maintains a constant magnitude in obtaining input current and the output voltage ripples without an increase in the number of components like an inductor, capacitor and filter circuits. The reliability of the MDIBC is increased as compared with other conventional converters due to several

factors, such as common heat sink, control scheme and mutual sharing of common DC link capacitor at the output, thus reducing shortcomings in terms of electrical faults and breakdowns. Furthermore, the overall efficiency as well as effectiveness are enhanced due to the utilization of regenerative braking power. In addition, the MDIBC is the preferred choice for high-power utilization in terms of interconnecting an HV battery to a DC link of an inverter. Nonetheless, the converter suffers from stability and sensitivity issues due to the transient state of the load current profile. Besides, the operation of the MDIBC is quite tricky to analyze under steady-state and transient conditions. Besides, components like a capacitor filter, heat sink and high-power inductor add extra weight to the converter [116–121].

Hegazy et al. [121] investigated the performance of the MDIBC for EVs using MATLAB/Simulink and accordingly built a TMS320F2808 DSP-based 30 kW prototype to validate the results through experiments. The simulation and experimental reports proved the superiority of the MDIBC topology over other DC-DC converters with respect to reliability and high performance. Chakraborty et al. [11] proposed an interleaved bidirectional DC-DC converter for EVs to achieve multi-objective targets between model functionalities, accuracy and execution time. The proposed interleaved converter was validated and optimized using a dSPACE SCALEXIO hardware-in-the-loop test bench with a minimal latency of 18  $\mu$ s. The result showed a difference of less than 1.25% in the accuracy between the modeling approach and test bench approach. Shang et al. [122] introduced interleaved parallel topology-based resonant LC converters to self-heat batteries in vehicular applications using a high-frequency sine-wave (SW) heater. Accordingly, a thermoelectric model was designed to determine the optimal parameters of the SW heater. The experimental results demonstrated that the proposed topology reduced the electrochemical heat, ohmic loss and heating time effectively.

The MDIBC topology is configured using two power sources, BSSs and SCs, where BSSs act as the main power source while SCs operate as the auxiliary power source, as shown in Figure 4e. The MDIBC can be termed as a multi-port multi-phase interleaved converter that utilizes an interleaving technique and employs two high-frequency switches [123]. The circuitry design of the MDIBC comprises multiple parallel switches per phase which are linked to the interleaving control strategy technique. Due to its bidirectional characteristic, switching signals are shifted by  $360^\circ / (N \times S)$  per phase [124]. The output of the converter is controlled by various controllers such as feedback linearization, conventional dual loop and state feedback. The expression of the duty cycle of the MDIBC is presented in the following equation [116,123,125–127]:

$$D = \frac{1}{N} \left( 1 - \frac{V_{in}}{V_{out}} \right) \quad (6)$$

### 3.2. Isolated Converter

The isolated bidirectional converter is designed using three primary phases, including DC/AC/DC. A high-frequency transformer (HFT) is utilized to lift the input voltage at higher values through the utilization of the intermediate AC stage. The HFT is responsible for providing galvanic isolation, leading to high voltage gain. The various isolated converters for EV applications are presented in the following sections.

#### 3.2.1. Push–Pull Converter

The DC-DC push–pull converter (PPC) topology in EV operation is based on the transformer action which transforms the power from one side of the circuit to the other side, i.e., primary to secondary. The PPC has various advantages, such as simplicity and higher efficiency due to lower peak current, resulting in lower conduction losses. Nonetheless, the PPC suffers from smaller filters as compared to other DC-DC converters. In addition, precautions are necessary while a switching operation is carried out since switches at the same time might potentially damage the converter due to the formation of a low impedance path and very high current [128].

Wu et al. [129] presented a modified voltage-fed three-phase DC-DC PPC for EV applications. The proposed configuration achieved low switching losses and high efficiency as compared with conventional three-phase topology. Hendra et al. [130] employed state-space averaging to design a PPC for vehicular applications. A control strategy is applied to obtain a soft-start mechanism that minimized the starting power and voltage peak on the primary side. The simulation outcomes demonstrated the feasibility of PPC topology in the EVs in obtaining high efficiency as well as low current and voltage harmonics at the output.

The operation in the DC-DC PPC for EVs is different from other topologies, such as a flyback converter that stores energy during the first phase of the switching sequence and then transfers the energy to the load in the next switching sequence. The circuit configuration of the PPC is designed using a rectifier diode, bypass capacitor, transformer circuit and power switches. The configuration of the bidirectional DC-DC PPC for an EV drivetrain comprises a rectifier diode, bypass capacitor, transformer circuit and four switches, S<sub>1</sub>, S<sub>2</sub>, S<sub>3</sub> and S<sub>4</sub>, which operate simultaneously, as shown in Figure 5a. The output voltage is regulated in a feed-forward manner by the transformer action. Furthermore, the output of the transformer is determined by the turn ratios. The necessity for a loop stabilization technique is eliminated due to well-regulated outputs. The working principle of the PPC consists of two modes, i.e., PUSH mode and PULL mode. When the converter is functioning in PUSH mode, switch S<sub>2</sub> is ON and current flows from the battery to S<sub>2</sub>. At the same time, current in the transformer flows through switch S<sub>4</sub> and the output capacitor. Similarly, when the converter is operating in PULL mode, switch S<sub>1</sub> is turned on and hence current transfers from the battery to S<sub>1</sub>. The flow of current through the output capacitor in both cycles is in the same direction, hence a positive output voltage is generated [131]. The expression for voltage gain in the DC-DC PPC is given as:

$$\frac{V_{out}}{V_{in}} = nD \quad (7)$$

### 3.2.2. Flyback Converter

The flyback converter (FC) is an isolated DC-DC converter that originates from the buck–boost converter consisting of an inductor split into the form of a transformer [132]. The energy is stored in the DC-DC FC during the ON state while energy is transferred in the OFF state [133]. The FC is primarily applied in low-power applications due to its cost-effectiveness, multiple isolated outputs, high output voltages and electrical isolation characteristics [134]. In addition, the FC eliminates inductive filters, thus saving cost and in turn providing filtered output. Furthermore, due to the elimination of freewheeling diodes, the FC can be utilized in applications with high load voltages compared with forward converters [135]. However, the FC possesses several disadvantages, such as high ripple current, high input capacitance and high losses.

Shen et al. [136] designed a DC-DC FC for EVs with a resistor, transformer and integrated circuit (IC). The performance degradation and system fault conditions were calculated based on the probability density distribution model. The model was validated through simulation and experimental works. Tseng et al. [137] developed an integrated derived boost–FC for an EV application. The proposed design integrated boost and an FC to obtain high voltage gain. Bhattacharya et al. [138] designed an FC for hybrid EVs which exhibited lower output current ripple, high gain and reduced leakage inductance. Sangeetha et al. [139] developed a multi-FC topology that incorporated lower leakage inductance to an acceptable limit.

A bidirectional DC-DC FC is configured for EVs containing two switches, two capacitors and a transformer for isolation purposes, as displayed in Figure 5b. The working principle of the FC takes place in two modes, i.e., switch ON operation and switch OFF operation. The transformer action takes place during the switch ON operational stage,

while creating a voltage across each side of the transformer. Accordingly, the magnetizing current for the closed switch operation becomes:

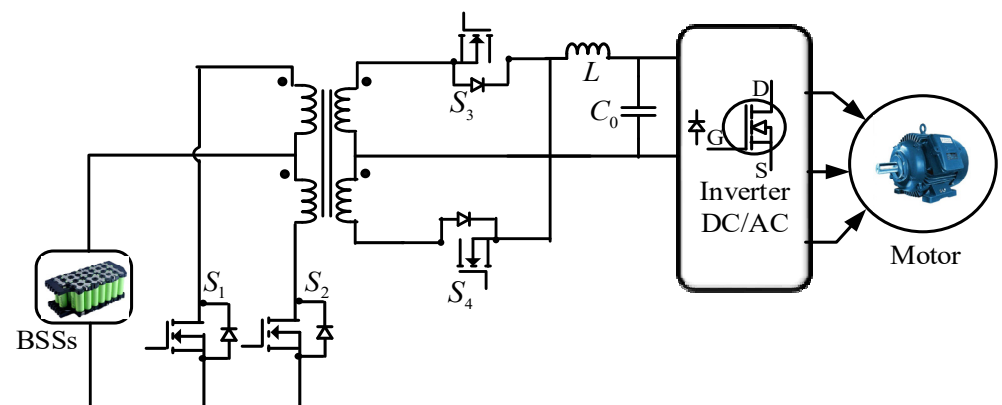
$$\Delta i_{L_{m_{closed}}} = \frac{V_s DT}{L_m} \tag{8}$$

$$V_s = V_p \frac{N_2}{N_1} \tag{9}$$

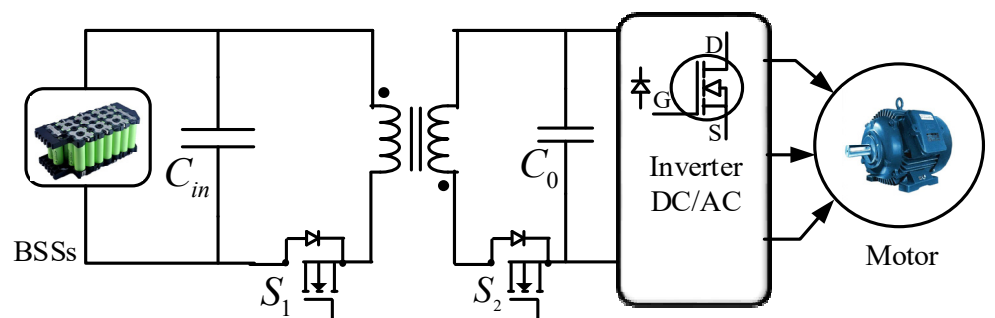
In contrast, the magnetizing current is generated during the switch ON operational stage, thus the open switch operation becomes:

$$\Delta i_{L_{m_{open}}} = \frac{-V_0(1-D)T}{L_m} \frac{N_1}{N_2} \tag{10}$$

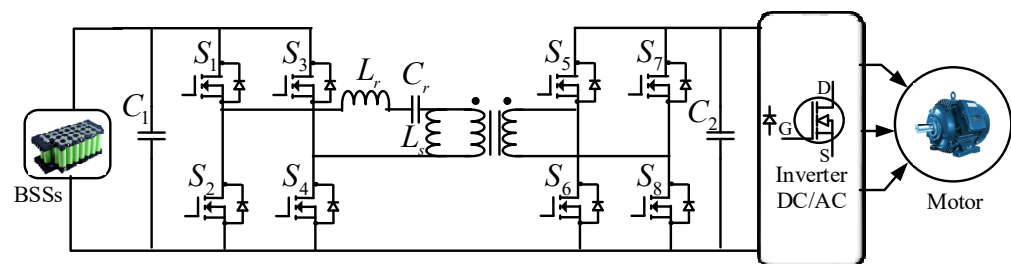
where,  $V_p$ ,  $V_s$  and  $V_0$  are the primary, secondary and output voltage, respectively.  $T$  is the total time duration,  $L_m$  is the magnetizing inductance.  $N_2/N_1$  is the turn ratio.



(a)



(b)



(c)

Figure 5. Cont.

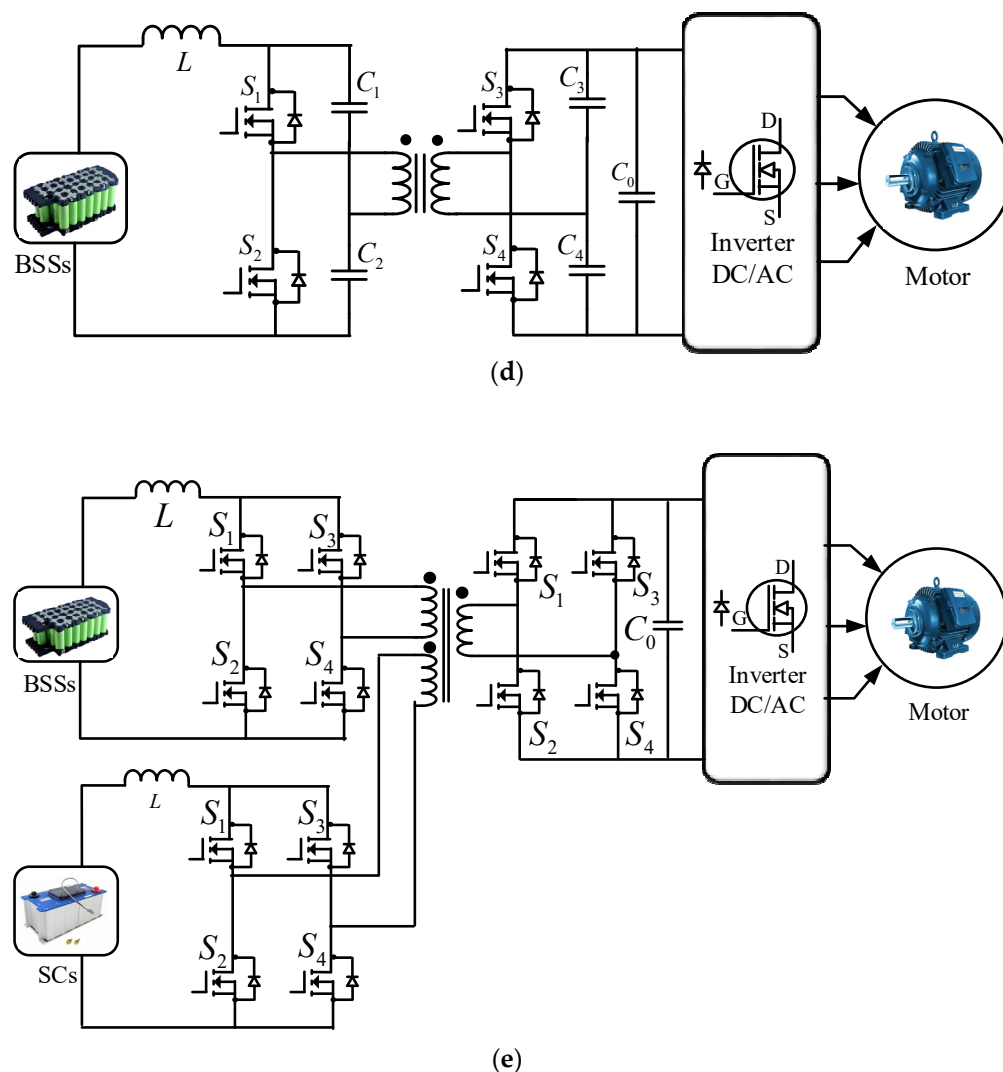


**Figure 5.** Configuration of isolated DC-DC converter for EVs: (a) push–pull converter, (b) flyback converter, (c) resonant converter, (d) zero-voltage switching converter and (e) multi-port isolated converter.

### 3.2.3. Resonant Converter

A DC-DC resonant converter (RC) for EV powertrain applications consists of a combination of inductors and capacitors which is known as the resonant tank. The resonant tank is utilized in tuning to resonance at a given frequency. The RC comprises four switches, four diodes and two resonant frequency components,  $L_r$  and  $C_r$ , as presented in Figure 5c. The magnetization inductance is used as the resonant element to execute the operation of the converter. Furthermore, the control in the RC under a no-load condition is resolved through the elimination of the magnetization current. The DC-DC RC for vehicular applications exhibits high efficiency and low switching loss [140]. In addition, other benefits, such as zero circulating current and zero voltage switching operation, provide better operation and efficiency for the battery charging profile [141]. Nonetheless, the RC has some limitations, such as heat problems due to magnetizing currents and complex design of the transformer [142].

Moradisizkoochi et al. [143] designed a modular topology using an RC converter based on Gallium Nitride (GaN) switches for EVs. The proposed design utilized enhancement-mode Gallium Nitride (eGaN) switches due to their high efficiency and switching speed. Furthermore, a 1 kW, 600 V, 100 kHz hardware design was set up to validate the design. Vu and Choi [144] employed a constant current and constant voltage (CV) charging mechanism to design a dual full-bridge LLC-based RC for EVs. The proposed converter achieved

higher accuracy with zero-voltage switching (ZVS) and zero-current switching (ZCS) under constant current charge operation for all the switches. Bai et al. [145] introduced a bidirectional DC-DC RC for EVs as well as vehicle-to-grid (V2G) applications over a wide range of voltage levels. It was concluded that the proposed DC-DC RC topology achieves higher efficiency and a high conversion ratio at low cost. The quality factor ( $Q$ ) and resonant frequency ( $F_r$ ) for the DC-DC resonant circuit are expressed as follows:

$$Q = \frac{\sqrt{L_r/C_r}}{R_{ac}} \quad (11)$$

$$F_r = \frac{1}{2\pi\sqrt{L_r C_r}} \quad (12)$$

### 3.2.4. Zero-Voltage Switching Converter

The zero-voltage switching converter (ZVSC) exhibits lossless switching, cold starting and contains less circuitry in comparison with other conventional converters for EV applications [146]. The ZVSC is appropriate for the EV drivetrain due to its components' reduced size, easy control technique and significant power density. Furthermore, the ZVSC can work without additional circuitry for soft switching and provide technical benefits, including friendly control methodology and higher efficiency [147]. Besides, the ZVSC needs less control and accessory power in comparison to the full-bridge component [148]. Nevertheless, the ZVSC experiences voltage stress across the switches in high-power applications. Furthermore, a large capacitor is required to limit ripples at the converter output. Due to the absence of a fault tolerance mechanism, the converter is not appropriate for operation above 10 kW [148–151].

Pahlevaninezhad et al. [151] introduced a novel full-bridge ZVSC in EVs to provide power effectively under varying load conditions. A current-driven rectifier was employed to execute the soft-switching operation, leading to a higher efficiency under all load settings. The validation was carried out using a 3 kW prototype and the experimental reports illustrated the superiority and feasibility of the ZVSC. Aamir et al. [152] proposed a high-gain ZVSC converter with a smaller number of switches for hybrid electric vehicles. The design consists of a voltage-clamped circuit, a coupled inductor and three active switches intended for the bidirectional operation of the converter. The ZVSC achieved an efficiency of 96% and 92% under boost operation mode and buck operation mode, respectively.

The design of the ZVSC includes dual half-bridge circuitries on the input side as well as the output side of the transformer, as depicted in Figure 5d. An inductor with BSSs followed by half-bridge switches is used to build the input side of the converter. The output side of the converter composes the remaining half-bridge switches and filter capacitor. A combination of switches and capacitors in parallel is required for the application of soft switching in the converter. The converter is operated in two different modes, boost mode and buck mode. The ZVSC works in boost mode when the power flows from the low-voltage side to the high-voltage side, while it operates in buck mode when the power transfers from high voltage to low voltage [148,153]. The equation of the duty cycle ( $D$ ) for the ZVSC is given as:

$$(1 - D) \times D = \frac{n \times V_{out}}{2V_{in}} \quad (13)$$

### 3.2.5. Multi-Port Isolated Converter

The multi-port isolated converter (MPIC) integrates the multiple input sources to extract the benefit of an individual source. The power recovered in the MPIC during the process of regenerative braking can be utilized to feed the power back to the input source, thus improving the efficiency as well as the functionality of the converter. Nonetheless, the MPIC has some shortcomings. Due to an increase in the number of switches, synchronization becomes difficult. Furthermore, the weight of the converter also increases due to the presence of a bulky transformer [154].

Zhao et al. [155] constructed three-port bidirectional DC-DC converters for EVs. The performance of the converter was improved using phase shift control, duty cycle control and overall system loss assessment. A controller-based converter model was designed and decoupled power flow management was executed to achieve a quick response in the dynamic state. The theoretical analysis was justified using a 1.5 kW prototype. The results demonstrated the suitability of the proposed topology in the EV drivetrain. Khan et al. [156] designed a smart electric vehicle charging station with multi-dimensional power flow capabilities by utilizing an isolated multi-port converter. The design was implemented in MATLAB/Simulink software and validated with a hardware prototype. In addition, the design suggests that EVs and energy storage batteries can be charged from the grid at the same time.

An isolated multi-winding transformer connects all the input ports, as displayed in Figure 5e. An interleaving technique is utilized to connect input sources as well as to minimize the input current and output voltage ripples. In addition, a parallel connection of two boost DC/DC converters is employed to combine various energy sources [157–159]. Table 1 illustrates the functional features and the number of components of the various DC-DC converters in EVs. A comparative analysis among the DC-DC converters in EVs is depicted in Table 2.

**Table 1.** Functional feature and component comparison between DC-DC converters in electric vehicle.

DC-DC Converter	Current/Voltage Ripple	Switching Frequency	Complexity of Control Circuit	High Power Conversion	EMI Suppression	Cost	Voltage Gain	Active Components			Passive Components	
								D	SW	HFT	L	C
CC	Simple	High	Simple	Appropriate	Reduced	Low	$\frac{-D}{1-D}$	2	2	0	2	2
SCBC	Moderate	High	Moderate	Appropriate	Needed	Medium	$\frac{2}{1-D}$	4	4	0	1	3
CIBC	Moderate	High	Moderate	Appropriate	Needed	Low	$\frac{2+n-D}{1-D}$	3	3	0	2	3
QZBC	Simple	High	Complex	Appropriate	Needed	Medium	$\frac{1+D}{1-D}$	3	3	0	2	3
MDIBC	Complex	Low	Complex	Appropriate	Reduced	Low	$\frac{1}{1-ND}$	16	16	0	4	1
PPC	Simple	High	Complex	Appropriate	Reduced	Low	$\frac{nD}{1-D}$	4	4	1	1	1
FC	Simple	High	Moderate	Not appropriate	Needed	Low	$\frac{nD}{1-D}$	2	2	1	0	2
RC	Simple	High	Moderate	Appropriate	Reduced	Low	$\frac{n 2\pi f_{sw} }{1-D}$	8	8	1	2	3
ZVSC	Complex	Low	Complex	Appropriate	Reduced	Medium	$\frac{2}{n}D(1-D)$	4	4	1	1	5
MPIC	Complex	Low	Complex	Appropriate	Needed	High	$\frac{n+1}{1-D}$	12	12	1	2	1

D is the number of diodes, SW is the number of switches, HFT is the number of high-frequency transformers, L is the number of inductances, C is the number of capacitances, n is the transformer turns ratio, N is the number of phases,  $f_{sw}$  is the switching frequency. CC: Cuk converter; SCBC: switched-capacitor bidirectional converter; CIBC: coupled inductor bidirectional converter; QZBC: quasi-Z source converter; MDIBC: multi-device interleaved bidirectional converter; PPC: push–pull converter; FC: fuel cell; RC: resonant converter; ZVSC: zero-voltage switching converter; MPIC: multi-port isolated converter; EMI: electromagnetic interference.

**Table 2.** Comparative analysis of various DC-DC converters used in EVs.

Type	Ref.	DC-DC Converter	Objective	Outcomes	Benefits	Drawbacks
Non-isolated converter	[92]	CC	-To prevent high energy loss.	-Provides stable and ripple-free output.	-Peak-to-peak ripple current of inductors is smaller. -Continuous input and output currents.	-Difficult to stabilize. -Uncontrolled and undamped resonance.
	[93]	SCBC	-To obtain high voltage gain and efficiency.	-Efficiency is greater than 90%.	-Cost-effective. -Compact design. -Current output limited.	-High ripple current. -Fails to maintain higher efficiency for a wide range of ratios of input to output voltages.
	[106]	CIBC	-To reduce output current and inductor current ripples.	-Increase in the efficiency by increasing coupling coefficient.	-Small size. -Low cost. -Reduced ripples.	-Limited scope for further improvement. -No consideration for voltage ripples.
	[112]	QZBC	-To obtain wide range of voltage gain, and an absolute common ground.	-Maximum and minimum efficiency are 96.44% and 88.17%, respectively.	-Lower switch stress. -Smaller component ratings. -Buck/boost capability.	-Input current is discontinuous. -Capacitor has high voltage stress.

Table 2. Cont.

Type	Ref.	DC-DC Converter	Objective	Outcomes	Benefits	Drawbacks
Isolated converter	[121]	MDBIC	<ul style="list-style-type: none"> <li>-To reduce the number of passive components.</li> <li>-To decrease the ripples in input current and output voltage.</li> <li>-To obtain proper control and fast transient response.</li> </ul>	<ul style="list-style-type: none"> <li>-Obtains low EMI and low stress.</li> <li>-Halves current and voltage ripple in comparison to interleaved boost converter (IBC).</li> <li>-Halves inductor and capacitor size compared to IBC.</li> </ul>	<ul style="list-style-type: none"> <li>-Low current stress.</li> <li>-High efficiency.</li> <li>-Ideal for high-power conversion.</li> <li>-Simple control approach.</li> <li>-Reduced heat sink and component size.</li> </ul>	<ul style="list-style-type: none"> <li>-Complex circuit due to the high number of components.</li> <li>-Duty cycle is very sensitive under load variation.</li> <li>-Study under steady-state and transient conditions is complex.</li> </ul>
	[130]	PPC	<ul style="list-style-type: none"> <li>-To change the voltage of DC power supply.</li> </ul>	<ul style="list-style-type: none"> <li>-Limits the starting power.</li> <li>-Achieves low current and voltage on the primary side.</li> </ul>	<ul style="list-style-type: none"> <li>-Better utilization of transistors and transformers.</li> <li>-Reduces EMI.</li> <li>-Less filtering required.</li> </ul>	<ul style="list-style-type: none"> <li>-Central tap transformer.</li> <li>-Two switches are not widely used in flux walking phenomena.</li> </ul>
	[139]	FC	<ul style="list-style-type: none"> <li>-To enable support of a wide input voltage range.</li> </ul>	<ul style="list-style-type: none"> <li>-Attains lower leakage inductance to an acceptable limit.</li> </ul>	<ul style="list-style-type: none"> <li>-Primary is isolated from the output.</li> <li>-Can provide multiple output voltages.</li> <li>-Ability to regulate the multiple output voltages.</li> </ul>	<ul style="list-style-type: none"> <li>-Has ripple current.</li> <li>-Higher losses.</li> <li>-More output and input capacitance.</li> <li>-Has the right half pole in the compensation loop.</li> </ul>
	[145]	RC	<ul style="list-style-type: none"> <li>-To minimize magnetic components and passive filters.</li> </ul>	<ul style="list-style-type: none"> <li>-Obtains high step-up/down capability.</li> <li>-Achieves high efficiency.</li> <li>-Attains wide voltage gain range.</li> </ul>	<ul style="list-style-type: none"> <li>-Low cost.</li> <li>-High conversion ratio.</li> <li>-High efficiency.</li> </ul>	<ul style="list-style-type: none"> <li>-Expensive controller.</li> <li>-Complex integrated transformer.</li> </ul>
	[151]	ZVSC	<ul style="list-style-type: none"> <li>-To provide satisfactory power under wide range load variations.</li> <li>-To perform the soft-switching with acceptable efficiency.</li> <li>-To clamp the output diode bridge voltage.</li> </ul>	<ul style="list-style-type: none"> <li>-Achieves zero voltage switching under all load conditions.</li> <li>-Ensures a stable and reliable process under no-load condition through the symmetric auxiliary circuits.</li> </ul>	<ul style="list-style-type: none"> <li>-Low EMI.</li> <li>-Low switching loss.</li> <li>-Additional clamping circuit is not required.</li> </ul>	<ul style="list-style-type: none"> <li>-Large capacitor is needed.</li> <li>-High current ratings.</li> <li>-Poor fault-tolerant capability.</li> </ul>
	[155]	MPIC	<ul style="list-style-type: none"> <li>-To control duty cycle to optimize the system behavior.</li> <li>-To minimize the overall system losses.</li> <li>-To investigate the dynamic analysis and related control strategy.</li> </ul>	<ul style="list-style-type: none"> <li>-Achieves a fast dynamic response.</li> <li>-Independent control of power flow.</li> <li>-Achieves high efficiency through duty cycle control and phase-shift control.</li> </ul>	<ul style="list-style-type: none"> <li>-High voltage gain.</li> <li>-Low output voltage ripple current.</li> <li>-Galvanic isolation.</li> </ul>	<ul style="list-style-type: none"> <li>-Large number of components.</li> <li>-Complex analysis under steady-state and transient conditions.</li> <li>-High sensitivity corresponds to duty cycle under load changes.</li> <li>-Difficult to achieve proper synchronization.</li> </ul>

#### 4. EV Converter Controller Schemes

DC-DC converters are nonlinear and exhibit lightly damped dynamics due to switching behavior [160]. Therefore, a suitable control technique of DC-DC converters is essential to obtain a regulated and fixed output voltage. The control of converters based on classical linear regulators, such as proportional–integral (PI) regulators, is available, however, the PI control strategy suffers from limited and unsatisfactory performance with a large load and system parameter variation [161]. To overcome these concerns, intelligent controllers are introduced due to their quick response, excellent dynamic performance and strong controllability. This paper summarizes the various control strategies and suggests the most viable solutions in EV applications.

##### 4.1. Proportional–Integral Control

The proportional–integral (PI) controller is based on a feedback control loop that estimates an error signal from the difference between the output of a system and a reference value. The PI controller provides zero control error and it is insensitive to the measurement channel, thus the PI controller can be used to increase the stability and to avoid large disturbances during the system operation [162]. The application of the PI controller in EV converters is illustrated in the following subsections.

#### 4.1.1. PI Controller in Battery Lifespan Improvement

A PI controller-based DC-DC converter mechanism is established for EVs employing multiple energy sources, including BSSs, SCs and FCs [156]. Advanced vehicle simulator software (ADVISOR) is proposed in this study considering the state of charge of the battery and supercapacitor, speed of the vehicle and power demand. Though FCs are taken as the main energy source, they exhibit poor efficiency during light loads, and thus rely on a battery to supply the power in this situation. The complementary switching is used in the battery converter to avoid discontinuous transition which further reduces the current peaks and saves the active and passive components from dangerous stresses. The overall lifespan of the battery and the temperature adaptability of the hybrid system are improved significantly. The battery maximum energy was calculated as:

$$Energy_{max} = \frac{Ah_{max} \cdot V_{nom} \cdot 3600 \text{ s/h}}{1000 \text{ J/kJ}} \quad (14)$$

where  $V_{nom}$  is the nominal voltage,  $R_{int}$  is the internal resistance and  $Ah_{max}$  denotes the maximum ampere-hour of the battery. However, optimal size and cost are not considered in this study.

#### 4.1.2. PI Controller in Stability Improvement of an Integrated Charging System

Kang et al. [163] discussed the PI control methods for DC-DC converters to enhance the stability of an integrated charging system in a hybrid EV (HEV). In this research, the feed-forward compensation method is employed to regulate the DC-link voltage and load current in the transient state, which improves the overall system stability. The advantage of this system is that it does not require additional capacitance, leading to a reduction in the system volume and cost. Figure 6 depicts the block diagram of the PI control-based DC-DC converter where the controller operation is executed in constant current (CC) and constant voltage (CV) modes. During CC mode, the operation of the DC-DC current controller depends on the reference current  $i_{Bt}^*$ , whereas during CV mode, the operation of the controller relies on the reference voltage  $v_{Bt}^*$ .

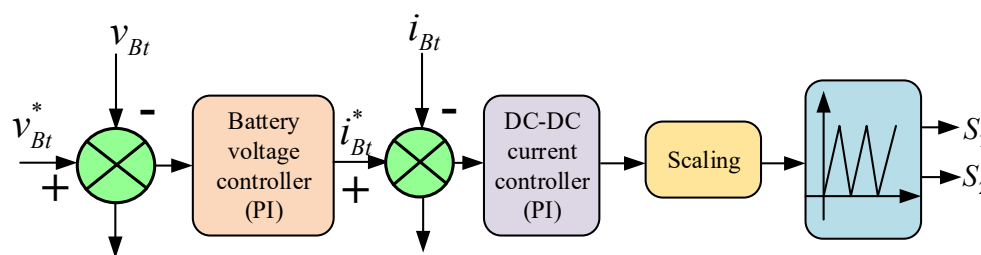


**Figure 6.** Block diagram of bidirectional mode operation of proportional–integral (PI)-based DC-DC converter [163].

#### 4.1.3. PI Controller in Universal Three-Level Bridge Converter

Al-Ogaili et al. [164] suggested a PI-based voltage-oriented control (VOC) scheme to control the universal three-level bridge converter through the control of input voltage and output current. The control architecture is shown in Figure 7. Here, the PI voltage controller controls the DC-link voltage ( $V_{DC}$ ) which is compared with a reference voltage,  $V_{dc\_ref}$  to estimate the reference current signal,  $i_{d\_ref}$ . The PI current controller minimizes the error between the reference current  $i_{d\_ref}$  and the inner loop of the active  $i_d$  current component to estimate the reference voltage signal,  $v_{d\_ref}$ . Similarly, the other PI controller manages to reduce the  $i_q$  current component to zero to estimate the reference voltage signal  $v_{q\_ref}$ . The active current component  $i_d$  is regulated by the DC-link voltage control approach that helps to balance the active power flow. On the other hand, the regulation of reactive component  $i_q$  to zero ensures the unity power factor operation. The steady-state error is reduced with this proposed system.

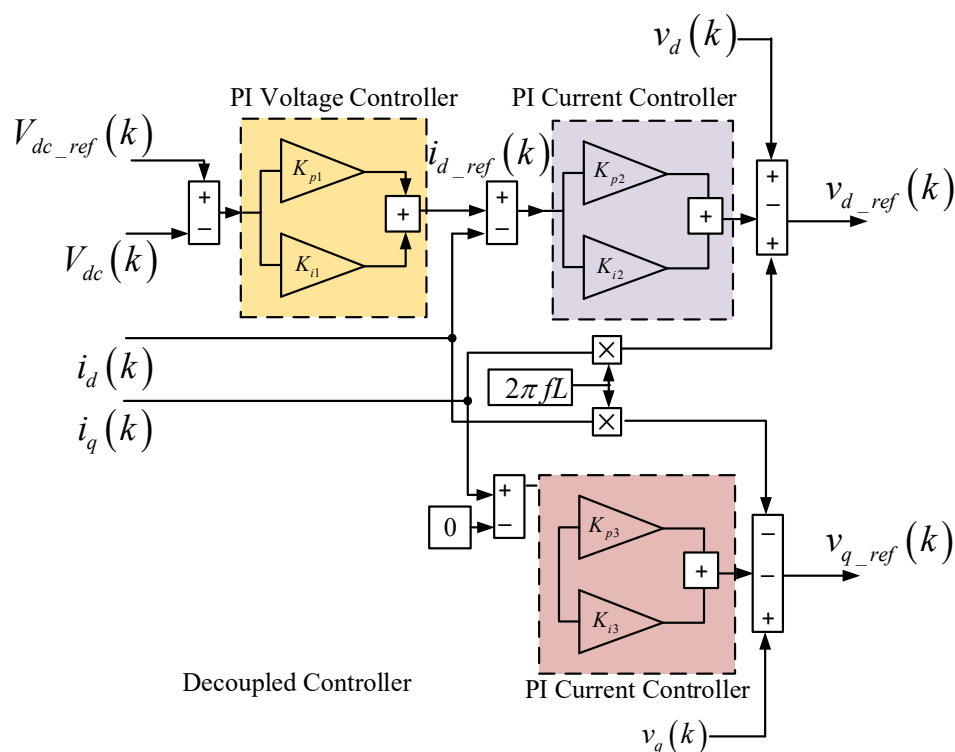


Figure 7. The control architecture of voltage-oriented control (VOC) control technique for EVs [164].

#### 4.1.4. PI Controller in a Bidirectional Interleaved Hybrid Converter

Saleeb et al. [165] proposed a PI controller in a dual-loop control strategy for a bidirectional interleaved hybrid converter (BIHC). It is evident from Figure 8 that the PI controller-based BIHC is designed to regulate the DC output voltage to a safe value. The amplitude of the input reference current ( $I^*$ ) of the proposed design is formed, which is then multiplied with the output of the phase-locked loop (PLL). The PI controller helps in tracing the inductor current ( $I_{L1}, I_{L2}, I_{L3}$ ) to the reference current and, accordingly, the appropriate gateway signals ( $G_{S1}$ - $G_{S6}$ ) are generated. This topology offers benefits in terms of fixed switching frequency, resulting in battery life improvement, higher processing capability and improved reliability [166].

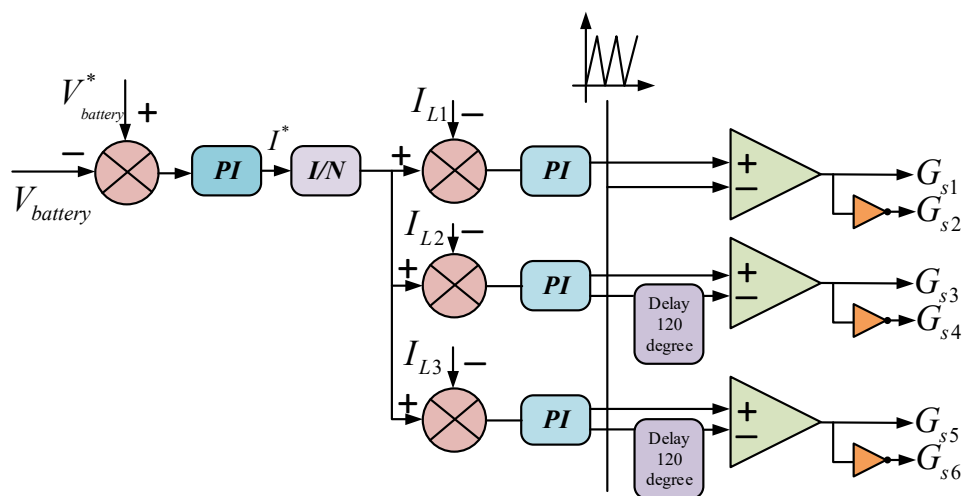


Figure 8. Schematic of a dual-loop control strategy based on the PI controller for a BIHC [165]. BIHC: Bidirectional interleaved hybrid converter.

#### 4.2. Rule-Based Control

The robustness and reliability of the rule-based controller depend on the specifications, designer knowledge, constraints and practical aspects. This section describes the various rule-based control techniques used in EVs.

##### 4.2.1. Fuzzy Logic Control

Ferreira et al. [167] suggested a fuzzy logic control (FLC)-based multiple-input power electronic converter (MIPEC) to attain high efficiency in EVs, as shown in Figure 9. The BSSs, SCs and FCs are used, where the input current is controlled by BSSs and the regulation of the DC-link voltage is performed by SCs. The battery energy load current and SCs are taken as the input of FLC, while the BSS output current correction and FCs are introduced as the output variables. The MIPEC interfaces between the DC-link bus, ESSs and generator. The power flow between the sources and load is coordinated by the fuzzy system while ensuring adequate operational conditions for the traction system. Although FLC provides satisfactory results, it does not confirm the optimal solution under different situations. Moreover, low-cost, flexible and efficient operation of MIPECs, including low EMI, is yet to be developed for EV applications. Adam et al. [168] proposed an FLC-based bidirectional converter in EVs to carry out the control operation of battery charging and discharging current, which provided higher capacity and longer lifespan. The simulation results demonstrated satisfactory outcomes of the converter with regard to stable output voltage and high operating efficiency. Narayana et al. [169] designed a bidirectional DC-DC converter topology based on FLC in EVs that illustrated cost-effectiveness, a smaller number of components and high efficiency.

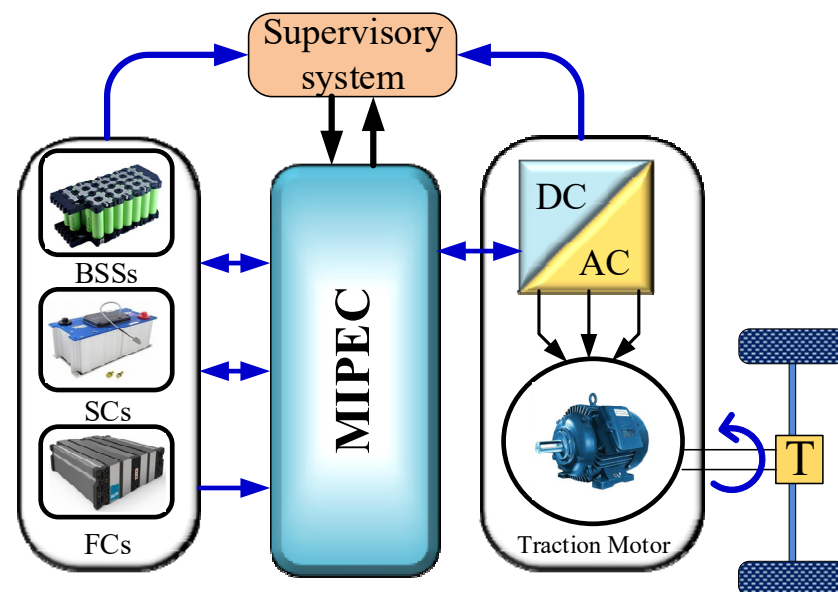


**Figure 9.** Block diagram of bidirectional mode operation of PI-based DC-DC converter [163]. MIPEC: Multiple-input power electronic converter

##### 4.2.2. Neuro-Fuzzy Logic Control

The adaptive neuro-fuzzy inference system (ANFIS) is the combination of both neural networks and fuzzy inference systems, and thus is quicker and more accurate than the traditional fuzzy system. Reddy and Sudhakar [170] designed an EV powertrain with FCs, a boost converter, three-phase inverter, motor and ANFIS controller, as denoted in Figure 10. An ANFIS-based maximum power point tracking (MPPT) controller is employed to extract the maximum energy from FCs. The proposed ANFIS controller demonstrates satisfactory performance in comparison to FLC, reducing the average time to reach the maximum power point by 17.74% and increasing the average DC-link power by 1.95%.

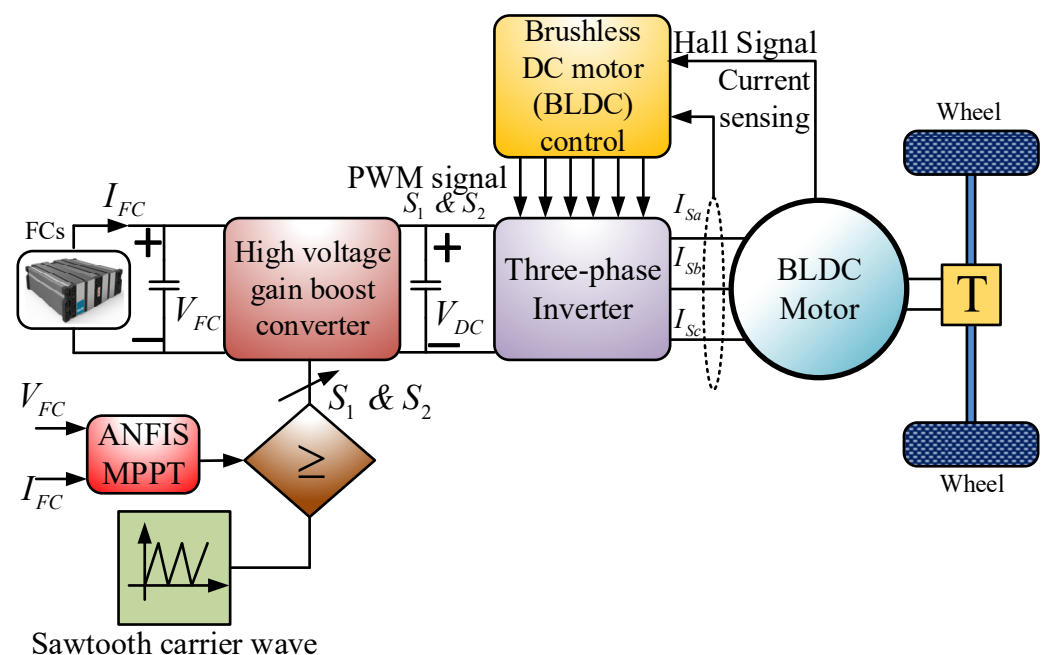


**Figure 10.** Boost converter based adaptive neuro-fuzzy inference system (ANFIS) maximum power point tracking (MPPT) controller for an EV system. Reprinted from [170] with permission from Elsevier.

#### 4.2.3. Fuzzy PI Control

An intelligent energy management system employing fuzzy PI energy for BSSs and SCs in an HEV is proposed in [171]. Here, the adaptive PI controller is used to prevent deep discharging or over-charging, and the fuzzy-based low pass filter is used for optimal power sharing. Both the control methods are responsible for adjusting the battery current based on the maximum current of the DC-DC converter. The output of the fuzzy system is fed to the proportional and integral gain of the PI controller. In [172], a multi-input DC-DC converter is designed based on fuzzy PI for EVs to obtain fast tracking capability as well as to control the bidirectional power management with fewer steady-state errors and proper utilization of energy sources. Here, the load demand, source status and the control switching signals are utilized to execute the operation of a buck–boost converter. The source-side average current mode control is executed by the PI controller which contains the inner current control loop and outer voltage loop. In the proposed method, the control operation of the inductor current is carried out by adjusting the individual source current for a specified load. A logical switching mechanism to alternate the control action between PI and fuzzy is proposed based on the speed error value (5 rpm in this case), as depicted in Figure 11. The PI controller operates below this limit and fuzzy operates above this speed error limit.

#### 4.3. Artificial Neural Network Control

Intelligent control based on an artificial neural network (ANN) for the half-bridge LLC resonant converter in EV applications is presented in [173]. The proposed topology achieves an excellent solution with regard to long battery lifespan and high energy efficiency, leading to obtaining more miles per charge in EVs. The performance of the ANN-based LLC resonant converter is evaluated using the mean square error (MSE). Here, the reference values are compared with the input voltage, load voltage and dynamic load values. The measured error value is controlled by switching frequency through the Levenberg–Marquardt training algorithm and the activation function of the ANN. Six different states of load are considered in this study. The results indicate that the ANN obtains peak efficiency, ripple voltage and THD of 96.2%, 0.5 V and below 5%, respectively. Teja et al. [174] proposed an ANN control-based bidirectional converter to execute power flow control under two operational processes, namely, the energy regeneration stage and

dual-source powering stage. The simulation outcomes demonstrated that the ANN control performed better than PI control in terms of fast response and reduced current ripple.

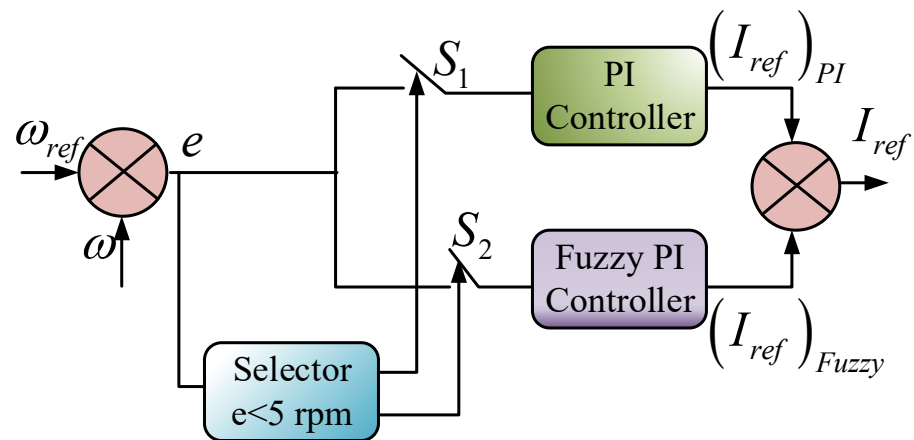


**Figure 11.** The block diagram of hybrid fuzzy PI controller for a DC/DC converter in an EV application [171].

#### 4.4. Sliding Mode Control

An adaptive sliding mode control (ASMC) scheme is applied to achieve the current tracking control for boost converters in EVs [175]. The control operation of ASMC is enhanced with optimal reaching law (EORL). The simulations and experimental results illustrate that EORL-based ASMC delivers better results than conventional ASMC methods in terms of stable power distribution, tracking control and convergence time [176]. In [177], a novel method utilizing sliding mode (SM) control-based buck–boost bidirectional converter is proposed. The DC-DC converter is designed. The proposed method does not require an additional sensor and demonstrates strong robustness under the changing input voltage and converter load. In [178], SMC is applied to address the harmonic issue of the bidirectional DC/DC converter in SCs for HEVs. In [179], an adaptive fractional order sliding mode control (AFSMC)-based boost converter is built to attain current tracking control for a hybrid storage system with BSSs and SCs. A Lyapunov function is developed using the adaptation rules and tracking current error. The simulation outcomes demonstrate the effectiveness of the proposed design over the conventional SMC system with regard to a fast transient response and robustness under uncertainties. Table 3 presents the operational feature comparison among various controllers. The comparative performance analysis of various control strategies used in EV drivetrains is presented in Table 4. Liu et al. [180] presented a novel coupled thermoelectric model to charge a LiFePO<sub>4</sub> battery using a constrained generalized predictive control (GPC)-based charging control strategy. The proposed model aimed to achieve fast charging as well as keep the internal temperature of the battery within an acceptable range. A controlled auto-regressive integrated moving average (CARIMA) model was built as a self-tuning model for the GPC controller, which was optimized by the recursive least squares (RLS) algorithm. Then the charging current was adjusted using the GPC controller under different control parameters, internal temperatures and heat dissipation rates. Ouyang et al. [181] introduced a leader–followers framework using an optimal charging control strategy with multi-objective optimization aiming to reduce the energy loss of a series-connected Li-ion battery pack and fulfill the user demand. The proposed framework integrated the online closed-loop regulation and offline scheduling to enhance the robustness and decrease the computational burden for the charger controller. The proposed charging control strategy was validated under different tests, including state of charge (SOC) settings, weight coefficients in the cost function and measurement noise and the results demonstrated the effectiveness in a real-world environment compared with those methods with complex battery models.

**Table 3.** Feature comparison of different controller strategies used in EV converters.

Feature	Proportional Integral (PI) Control	Fuzzy Control	Artificial Neural Network (ANN) Control	Sliding Mode (SM) Control
Control operation	Linear	Artificial intelligence	Artificial intelligence	Non-linear
Control complexity	Medium	Less	High	High
Mathematical modeling	Required	Not required	Not required	Required
Sensitivity	High	Low	Low	Low
Dynamic response	Average	Excellent	Excellent	Good
overshoot	Large	Negligible	Negligible	Negligible
Control suitability	Lower order systems	All types of system	All types of system	All types of system
Capability to handle complexity	Difficult	Very easy	Easy	Easy

**Table 4.** The comparative study of various control methods employed in converters of EVs.

Ref.	Control Technique	Target	Contributions	Advantages	Disadvantages
[164]	PI control	-To control input voltage and output current. -To reduce the error between the reference current and the inner loop of the active current component.	-Manages to reduce the current component to zero. - Helps to balance the active power flow. - Ensures unity power factor operation.-Reduces the steady-state error.	-Easy execution. -Simple design. -Unstable operation due to inappropriate tuning.	-Needs precise mathematical modeling. -Inappropriate for highly non-linear, time-varying systems. -Poor transient response under a time-delayed system.
[167]	Fuzzy control	-To control peak current, voltage and average power demand. -To achieve high efficiency. -To interface between ESSs, generator and the voltage DC-link bus.	-Proper coordination between ESSs, including BSSs, SCs, FCs and load. - Confirms sufficient conditions for traction system operation.	-Robust, flexible, smooth and fast response. -Minimizes voltage and current ripple. -Improves dynamics and excellent transient response. -Can handle non-linear systems and work with imprecise inputs.	-Needs expert knowledge to design the controller. -Generation of fuzzy rules is a laborious task. -Needs frequent upgrades of fuzzy rules.
[173]	ANN Control	-To achieve high power factor, low harmonics of input current and high efficiency. -To obtain a higher battery life expectancy.	-Obtains peak efficiency, ripple voltage and total harmonic distortion (THD) of 96.2%, 0.5 V and below 5%, respectively.	-Accurate and robust. -Flexible controllability. -Improved transient response. -Satisfactory operation under varying loads.	-Suffers from computational complexity problems. -Not ideal for fast switching operations. -Needs expensive processor devices.
[179]	SM control	-To attain current tracking control.	-High robustness. -Minimizes 80% of the transient time during the startup condition. -Allows the ESSs to reach a steady-state condition promptly.	-Reliable and robust. -Excellent dynamic response. -Easy execution. -Improved stability.	-Switching frequency fluctuates under voltage and load variation. -Frequency variation affects the design process of input and output filters. -Selection of appropriate parameters is challenging due to the high control complexity.

#### 4.5. Modulation Techniques in EV Converters

The modulation technique is vital for EV converters in achieving high efficiency, low switching losses and THD. Different modulation schemes are employed to control DC-DC converters in EV applications. The purpose of using the modulation techniques is to obtain the optimum point toward achieving the target amplitude, frequency and phase of the current and voltage [182,183]. The most widely used modulation scheme used in EV applications is pulse-width modulation (PWM). The modulation schemes used in different DC-DC inverters for EV applications are presented in Table 5. For instance, Zhang et al. [112] designed the PWM-based QZBC in EV applications to generate three gate signals in the step-up mode and step-down mode. Hegazy et al. [121] proposed an MDIBC integrated with TMS320F2808 DSP based on PWM to implement dual-loop current control in EVs. Shen et al. [136] employed an improved numerical model and fixed frequency pulse-width modulation (FFPWM) to evaluate the electromagnetic interference (EMI) performance of EVs. Pahlevaninezhad et al. [151] used a ZVSC and TMX320F28335 eZdsp with six enhanced pulse-width modulation modules to obtain a high-resolution PWM signal.

**Table 5.** Analysis of different modulation methods in EV converters.

Type	Converter	Authors	Modulation Techniques	Remarks
Non-isolated converter	CC	Pandey and Singh [91]	Pulse-width modulation	The authors proposed pulse-width modulation (PWM) control-based Cuk converter to achieve harmonic free input current in EVs. The outer loop is designed by the DC link control while the internal current control loop is formed using the input inductor current feedback.
	SCBC	Zhang et al. [96]	Pulse-width modulation	The authors employed PWM schemes in SCBC converters for EVs to generate the gate signals in the step-up mode and step-down mode.
	CIBC	Salehahari and Babaei [184]	High-frequency pulse-width modulation	The authors used the high-frequency PWM method in a CIBC to obtain the effective switching frequency as well as produce the desired output voltage and reduce switching stresses.
	QZBC	Zhang et al. [112]	Pulse-width modulation	The authors designed the QZBC with PWM generator for EVs to produce three gate signals in the step-up mode and step-down mode.
	MDIBC	Hegazy et al. [121]	Pulse-width modulation	The authors suggested closed-loop control to develop an MDIBC based on PWM. Here, the authors used TMS320F2808 DSP-based real-time digital control synchronized with PWM to execute the dual-loop current control.
Isolated converter	PPC	Hendra et al. [130]	Pulse-width modulation	The authors proposed a microcontroller-based control algorithm to generate a PWM duty cycle for an insulated-gate bipolar transistor (IGBT) using the date driver.
	FC	Shen et al. [136]	Fixed frequency pulse-width modulation	The authors employed fixed frequency pulse-width modulation (FFPWM) to assess the electromagnetic interference (EMI) performance of the FC in EVs using the improved numerical model.
	RC	Moradisizkoohi et al. [143]	Quasi-resonant pulse-width modulation	The authors suggested quasi-resonant PWM (QRPWM) where the switching frequency is higher than the resonant frequency. The proposed QRPWM showed better performance with regard to lower turn-off loss.
	ZVSC	Pahlevaninezhad et al. [151]	Enhanced pulse-width modulation	The authors developed TMX320F28335 eZdsp with six EPWM modules not only to generate a high-resolution PWM signal and high degree of flexibility but also to limit instability.
	MPIC	Zhao et al. [155]	Modified pulse-width modulation	The authors utilized controllers and a decoupling network and three duty cycle lookup tables along with 100 kHz PWM patterns to adjust the two-phase shift angle lookup tables.

## 5. EV Converter Optimization Algorithms

The optimization plays a key role in enhancing the converter efficiency through the reduction of converter loss and the minimization of ripple currents. Based on the literature review, optimization of the converter is classified into two groups: derivative information-based gradient methods and stochastic search-based metaheuristic methods.

### 5.1. Gradient Algorithms

The gradient-based algorithms are mathematically driven algorithms that are developed using rigorous mathematical expressions and thus the computational complexity is increased when variables increase. In [185], a Lagrange optimization function is formulated to optimize the size of the capacitors while fulfilling the constraints of total energy limit or total capacitance. The optimization also aims to find the optimal number of switch sizes to meet the constraints, including total switch volt-ampere (V-A) products or total switch conductance. In [186], sequential quadratic programming is utilized to reduce the total component cost of a boost converter while specifying several constraints, including ripple current, EMI standard, temperature switching frequency, physical configuration and safe operation procedures. Nevertheless, the main issue of gradient methods is the design space, which has numerous local minima and there is a chance of becoming trapped in a local minimum. Hence, gradient methods are unable to achieve global optimization solutions [187].

### 5.2. Metaheuristic Algorithms

The metaheuristic approaches are applied to address multi-objective and derivative-free problems with a large number of variables. A few studies have reported the use of optimization techniques in EV converter applications. Among various metaheuristic-based optimization methods, a genetic algorithm (GA) and particle swarm optimization (PSO) are extensively used for the design and optimization of the converter in EVs. Nguyen et al. [43] proposed GA optimization-based three-phase dual active bridge (DAB) bidirectional converters for EVs. The purpose of this method is to maximize the system efficiency by reducing the converter loss with low output current ripple. The heuristic GA is chosen due to its simplicity and feasibility. The optimization procedure affects the four basic parameters, the including leakage inductance ( $L_k$ ), peak flux density ( $B_{pk}$ ), voltage conversion ratio ( $M$ ) and switching frequency ( $f_s$ ) of the transformers. Hence, the minimization problem can be written as:

$$f(f_s, L_k, M) = \Delta P_{tot} \rightarrow \min \quad (15)$$

where  $\Delta P_{tot}$  denotes the total converter loss. The framework of the GA optimization is shown in Figure 12.

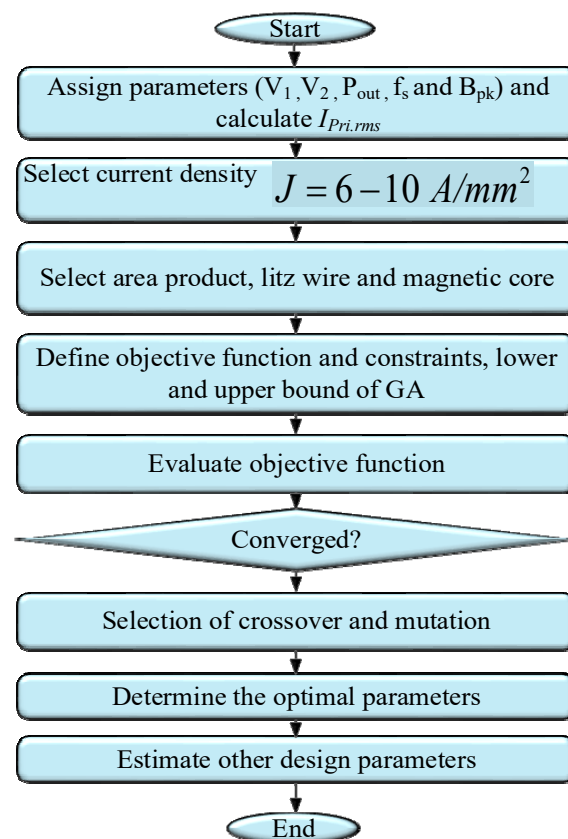


**Figure 12.** The methodological framework of genetic algorithm (GA) optimization to reduce converter loss [43].

First, the input voltage ( $V_1$ ), output voltage ( $V_2$ ), output power ( $P_{out}$ ), switching frequency ( $f_s$ ) and peak flux density ( $B_{pk}$ ) are assigned. Afterwards, the root mean square (rms) value of the primary current of the transformer is determined. Then, the fitness function is evaluated while satisfying the constraints of optimization. If the optimal parameters are obtained, then the designed parameters are calculated to reduce the converter loss, otherwise, the fitness function needs to re-evaluate to achieve the desired results.

An improved design methodology based on a non-dominated sorting GA-II (NSGA-II)-based DC-DC MPIC is presented to increase the effectiveness of the converter and minimize the development time [83]. The optimization problem is formulated to determine the optimal switching frequency and the number of phases. The results illustrate the superiority of the proposed method over the conventional method with regard to inductor weight, total loss of the converter and input current ripple. The multi-objective function can be mathematically expressed using the following equations:

$$\text{minimize} \begin{cases} \Delta I_{in}(X) \\ W_{\Sigma ind}(X) \\ P_{loss}(X) \end{cases} \quad (16)$$

$$\text{s.t.} \begin{cases} N_{ph\_min} \leq N_{ph} \leq N_{ph\_max} \\ f_{sw\_min} \leq f_{sw} \leq f_{sw\_max} \\ \Delta I_{in\_BAT} \leq 7.5\% I_{in\_BAT} \\ \Delta I_{in\_sc} \leq 20\% I_{in\_sc} \\ W_{\Sigma ind} \leq 5 \text{ kg} \\ P_{BCM} \leq 5 \text{ kW} \end{cases} \quad (17)$$

where  $\Delta I_{in}$ ,  $W_{\Sigma ind}$  and  $P_{loss}$  denote the input current ripple, inductor weight and converter loss, respectively,  $N_{ph}$  denotes the number of phases,  $P_{BCM}$  is the power of the boundary condition mode (BCM),  $f_{sw}$  represents the switching frequency,  $\Delta I_{in\_BAT}$  and  $\Delta I_{in\_sc}$  represent the input current ripple associated with the battery and supercapacitor, respectively.

Prithivi and Sathyapriya [84] designed a fuzzy controller with errors, and change of error as inputs and duty cycle as output. The proposed fuzzy controller minimizes the output voltage ripple of an isolated DC-DC converter. The effectiveness of the fuzzy controller is further enhanced by applying PSO and ant colony optimization (ACO). PSO and ACO obtain the optimum switching angle through the elimination of the ripple components. The results show that a closed-loop ACO-based fuzzy controller has lower output voltage ripple than PSO, at 0.14 V. The objective function of the proposed method is designed as:

$$f(d) = V_{ref} - V_{avg} \quad (18)$$

where  $V_{ref}$  denotes the reference voltage and  $V_{avg}$  is the average voltage. Liu et al. [188] proposed an ensemble multi-objective biogeography-based optimization (EM-BBO) approach to obtain an appropriate charging pattern for lithium-ion batteries. The authors formulated a multi-objective function to achieve three objectives simultaneously, including battery health status, energy conversion efficiency and charging time, while current, voltage, temperature and SOC were taken as constraints. The comprehensive analysis and results proved that the proposed optimization algorithm delivered a desirable trade-off between conversion efficiency and charging speed under different operational settings. Liu et al. [189] designed a coupled electrothermal-aging model based on the constrained multi-objective optimization framework to capture the lithium-ion battery dynamics, including aging and electrical and thermal characteristics. Two contradictory objectives, battery average temperature and charging duration, were taken into account subject to satisfying all constraints, including current, voltage, temperature and SOC. The NSGA-II approach was utilized to optimize of the multi-stage constant current (MCC) profile as well as assess the battery energy loss and economic management. The effectiveness of the charging management was examined using sensitivity analysis and various charging tests. The reports demonstrated the appropriateness of the proposed charging management with regard to the minimum economic cost of charging and suitable charging speed. Table 6 shows the summary of optimization algorithms used for EV converters.

**Table 6.** Surveyed literature on various metaheuristic optimization techniques for EV converters.

Algorithm	Ref.	Objective Function	Topology	Considered Factors	Outcomes
Genetic algorithm (GA)	[43]	-Maximizes the system efficiency.	-Bidirectional dual active bridge (DAB) converter.	-Leakage inductance, peak flux density, voltage conversion ratio and switching frequency.	-Eliminates the need for external inductors.
Non-dominated Sorting Genetic Algorithm II (NSGA-II)	[83]	-Minimizes the losses in the converter.	-Multi-objective, DC-DC multiport converters.	-Voltage and ripple current.	-Reduces the size, development time and input current ripple.
Particle swarm optimization (PSO)	[84]	-Switching angle optimization.	-KY boost converter.	-Voltage.	-Ripple current is reduced.
PSO	[85]	-Optimization of energy consumption.	-One-way DC-DC converter.	-Fuzzy membership functions are optimized.	-Reduces the influence of fuzzy control strategy.

## 6. Issues and Challenges

Although considerable efforts have been made toward the development of a converter with respect to design, control and optimization, numerous key issues need to be studied to enhance the accuracy and performance under various conditions. The key issues and challenges for converters are presented below.

### 6.1. Converter Design and Performance

The selection of the ideal converter topology is crucial for vehicle performance enhancement. The outcome of the vehicle may be unsatisfactory if a suitable design and topology of the converter are not chosen based on the requirements. A converter may be bulky due to a large number of passive parameters and switching components. Besides, the cost of the converter may increase due to the presence of an additional filter. In line with these, the converter may have several issues that may hamper the effectiveness, such as high voltage gain, high ripple current, switching loss, voltage stress, hard switching, inappropriate synchronization, high impedance and complex control techniques. Therefore, designing an effective converter is a challenge and a lot of factors need to be investigated.

### 6.2. Conventional Controller Issues

Although a conventional controller like a PI controller has a simple design, easy execution and provides reasonable performance, it has some weaknesses. For instance, a PID controller needs precise mathematical modeling which is very sensitive to load disturbance, changing environmental settings and parameter fluctuation. Besides, a PID controller delivers poor results for highly non-linear and time-varying systems. In addition, the PID controller has a slow transient response under a time-delayed system.

### 6.3. Intelligent Controller Issues

Intelligent controllers such as the fuzzy controller and ANN controller have shown promising results toward accurate and robust control of EV converters. However, they have some drawbacks. The fuzzy controller features flexibility, robustness, good transient response and easy hardware implementation, and is thus highly recommended for EV converter control. However, the fuzzy controller requires lots of data, human expertise and the frequent upgrading of rules. An ANN is robust, efficient and does not require mathematical modeling. Additionally, an ANN works satisfactorily under variable load conditions and changing parameters of the circuit. However, an ANN requires a huge amount of quality data for training and a large storage device. SM control presents a stable, reliable and robust solution. Additionally, SM control has an improved stability and dynamic response. However, SMC has issues of switching frequency fluctuation and suitable parameter selection.

#### 6.4. Optimization Algorithm Issues

Although the inclusion of optimization into EV converters has had considerable impacts with regard to design, cost and efficiency, it has some negatives concerning parameter selection, epoch number, data size and dimension settings. A GA has an easy implementation process and can perform a parallel search into multiple regions but suffers from slow convergence speed. In contrast, PSO requires fewer parameters to be adjusted and exhibits simple execution, high efficiency and fast convergence speed. However, PSO can converge prematurely and has difficulties in defining the initial design parameters. Hence, the choice of proper optimization technique is crucial to reach satisfactory solutions in converter control in EVs.

#### 6.5. Formulation of Multi-Objective Function

The formulation of the objective function is important to design robust optimization in vehicular applications. However, the construction of an objective function, considering many variables and constraints, is a challenging task. Generally, many parameters need to be optimized in converters, such as ripple current, voltage, switching loss, number of components and cost. To achieve these targets simultaneously, the formation of a multi-objective function is necessary. Nevertheless, it is tricky to obtain two optimal self-contradictory objectives concurrently without making one worse. For example, there is a lower possibility that ripple current and number of components will be optimized at the same time. Thus, the development of a multi-objective function and associated constraints is yet to be explored.

#### 6.6. Implementation of the Metaheuristic Algorithm

The execution of metaheuristic optimization in controlling the converter of EVs may deviate due to the highly mathematical computation and many algorithm parameters, functions and constraints. The training process of optimization is complex and needs a substantial amount of time. Besides, the performance comparison among various optimization techniques using a single convergence curve is a tough task. In addition, the integration of optimization may lead to poor results if a sufficient quality and quantity of data, data pre-processing, appropriate training algorithms and activation functions are not chosen accurately. Thus, further attention is required to address the computational complexity of the metaheuristic algorithm.

#### 6.7. Optimized Controller Design

The efficiency of an intelligent controller depends strongly on input features, network configuration and hyperparameter adjustment. The efficient and robust performance of the converter is ensured only when all the hyperparameters are optimized accurately. Several research works have ignored the membership function and hyperparameter tuning in fuzzy and ANN controllers, respectively. In the majority of cases, the intelligent controller is structured by adjusting the hyperparameters based on the trial and error (TE) method, contributing a substantial loss of time and human energy. Therefore, the appropriate architecture and hyperparameter settings of intelligent controllers are the key issues to be researched.

### 7. Conclusions and Suggestions

This review delivers comprehensive information and analysis of power electronic converters for EV drivetrains, concentrating on the converter, controller, modulation and optimization. As the first contribution, this review delivers a detailed insight into various advanced and viable DC-DC converter topologies in EV drivetrains with regard to their design aspects, operation, key features, advantages and disadvantages. In the case of non-isolated converters, CC offers wide-ranging voltage gain, however, it has limited power conversion efficiency due to the cascaded structures. The SCBC has enhanced conversion efficiency but has the limitation of high ripple current. The CIBC has a compact design and

has limited output current but it has the drawback of leakage inductance. Although the QZBC has extensive voltage gain, it has high voltage stress on capacitance. The MDIBC has become the preferred choice in vehicular applications in achieving low ripple current and voltage, high reliability, efficiency and high-power handling ability; nevertheless, it needs additional components and complex control techniques. On the contrary, among the isolated converters, the PPC has low conduction loss but has the drawbacks of smaller filters and high current. The FC can regulate multiple output voltages; nonetheless, it has more EMI and ripple current. The RC provides better operation and efficiency; however, it has a complex transformer design and limited capacity to carry magnetizing current. The ZVSC has low switching loss and EMI, but it has weaknesses in terms of high current ratings and unsatisfactory fault-tolerant ability. The MPIC has high voltage gain; nonetheless, it has issues of a larger number of components, ripple current, complex analysis and high sensitivity.

As the second contribution, this review also explores the various controller techniques to enhance the performance of EV converters. The control operation, contributions, benefits and shortcomings are presented explicitly. PI control has easy implementation but has poor performance in a non-linear, time-varying system. The intelligent controller is accurate, robust and has improved dynamic and transient response. Nevertheless, it is complex and requires human expertise. As a third contribution, the role of optimization in EV converters is investigated. In line with that, this review explores the different PWM techniques used in EV converters toward achieving desired current and voltage values. As a fourth contribution, the different metaheuristic algorithms concerning the process, objective function and constraints are highlighted. As a fifth contribution, the numerous key issues and challenges are identified related to converter topology, intelligent and optimization controller performance issues, optimized controller design and the formulation of a multi-objective function. As the sixth contribution, this review proposes some selective future research works for the advancement of EV operation, as follows:

- Generally, the converter exhibits high switching loss and power loss in the passive components. Currently, semiconductor materials including silicon carbide (SiC) and gallium nitride (GaN) have become increasingly popular due to their ability to handle high voltage and high current as well as provide high power density with low heat dissipation. However, they have issues of reliability and cost. Thus, future research works should be conducted on the appropriate material selection of the converter that can deliver cost-effective components with a high switching frequency, high reliability and low thermal loss.
- The topologies of the existing converters face problems such as high ripple current, low impedance, low voltage and current stress and sensitive duty cycle. Hence, further exploration is required on electrical design optimization to achieve high frequency and low converter loss under high-temperature conditions. In line with that, further investigation of mechanical design optimization of the converter is required to obtain high reliability, modularity, power density and efficiency.
- The multi-level multi-phase bidirectional converters have drawn attention due to their low current stress, simple control approach and high efficiency. Nonetheless, they need high component counts and complex analysis under steady-state and transient conditions. Besides, the duty cycle is very sensitive under load variation. Thus, it is recommended to focus on building a modular design framework to enable scalability, multi-functionality and high fidelity.
- Intelligent control techniques are useful to control the DC-link voltage and load current as well as achieve bidirectional power management, proper co-ordination of ESSs, fast tracking, fewer steady-state errors and high efficiency. However, they have drawbacks in terms of data integrity, long training operations, expensive processing devices and the need for suitable parameter selection and hyperparameter tuning. Therefore, further investigation is required to address the computational complexity.

- Although optimization algorithms are advantageous toward reducing converter loss, the number of components and cost, their execution in EV converters has been very limited. To date, only GAs and PSO have made decent progress to optimize the design and cost of the converter. Hence, it is suggested to utilize the advanced optimization algorithms in EV converter design.

The abovementioned suggestions could play remarkable roles in developing and executing advanced converters in EV applications. Moreover, this review can deliver an explicit idea and information to researchers and automotive engineers on converter configurations, control and optimization. Overall, this review helps to achieve a pathway for future sustainable EV expansions.

**Author Contributions:** Conceptualization, methodology, validation, investigation, visualization, M.S.H.L.; writing—original draft, M.S.H.L., M.F. and S.A.; writing—review and editing, M.A.H., A.H., A.A., M.H.M.S., T.F.K. and M.S.M.; funding acquisition, M.S.H.L. and A.H. All authors have read and agreed to the published version of the manuscript.

**Funding:** This research received funds from the Universiti Kebangsaan Malaysia with the project code of DIP-2018-020.

**Conflicts of Interest:** The authors declare no conflict of interest.

## References

- Hannan, M.A.; Lipu, M.S.H.; Hussain, A.; Mohamed, A. A review of lithium-ion battery state of charge estimation and management system in electric vehicle applications: Challenges and recommendations. *Renew. Sustain. Energy Rev.* **2017**, *78*, 834–854. [CrossRef]
- Hou, F.; Chen, X.; Chen, X.; Yang, F.; Ma, Z.; Zhang, S.; Liu, C.; Zhao, Y.; Guo, F. Comprehensive analysis method of determining global long-term GHG mitigation potential of passenger battery electric vehicles. *J. Clean. Prod.* **2020**, 125137. [CrossRef]
- Ameyaw, B.; Yao, L.; Opong, A.; Agyeman, J.K. Investigating, forecasting and proposing emission mitigation pathways for CO<sub>2</sub> emissions from fossil fuel combustion only: A case study of selected countries. *Energy Policy* **2019**, *130*, 7–21. [CrossRef]
- Lipu, M.S.H.; Hannan, M.A.; Hussain, A.; Hoque, M.M.; Ker, P.J.; Saad, M.H.M.; Ayob, A. A review of state of health and remaining useful life estimation methods for lithium-ion battery in electric vehicles: Challenges and recommendations. *J. Clean. Prod.* **2018**, *205*, 115–133. [CrossRef]
- IEA. Tracking Transport 2020. Available online: <https://www.iea.org/reports/tracking-transport-2020/electric-vehicles> (accessed on 12 September 2020).
- EEA. Greenhouse Gas Emissions from Transport in Europe—European Environment Agency. Available online: <https://www.eea.europa.eu/data-and-maps/indicators/transport-emissions-of-greenhouse-gases/transport-emissions-of-greenhouse-gases-12> (accessed on 15 May 2020).
- Hu, Y.; Wang, Z.; Li, X. Impact of policies on electric vehicle diffusion: An evolutionary game of small world network analysis. *J. Clean. Prod.* **2020**, *265*, 121703. [CrossRef]
- Xue, M.; Lin, B.-L.; Tsunemi, K. Emission implications of electric vehicles in Japan considering energy structure transition and penetration uncertainty. *J. Clean. Prod.* **2021**, *280*, 124402. [CrossRef]
- Asadi, S.; Nilashi, M.; Samad, S.; Abdullah, R.; Mahmoud, M.; Alkinani, M.H.; Yadegaridehkordi, E. Factors impacting consumers' intention toward adoption of electric vehicles in Malaysia. *J. Clean. Prod.* **2020**, *282*, 124474. [CrossRef]
- Feng, S.; An, H.; Li, H.; Qi, Y.; Wang, Z.; Guan, Q.; Li, Y.; Qi, Y. The technology convergence of electric vehicles: Exploring promising and potential technology convergence relationships and topics. *J. Clean. Prod.* **2020**, *260*, 120992. [CrossRef]
- Chakraborty, S.; Mazuela, M.; Tran, D.D.; Corea-Araujo, J.A.; Lan, Y.; Loiti, A.A.; Garmier, P.; Aizpuru, I.; Hegazy, O. Scalable Modeling Approach and Robust Hardware-in-the-Loop Testing of an Optimized Interleaved Bidirectional HV DC/DC Converter for Electric Vehicle Drivetrains. *IEEE Access* **2020**, *8*, 115515–115536. [CrossRef]
- Cao, C.; Chen, B. Generalized Nash equilibrium problem based electric vehicle charging management in distribution networks. *Int. J. Energy Res.* **2018**, *42*, 4584–4596. [CrossRef]
- Ding, X.; Wang, Z.; Zhang, L.; Wang, C. Longitudinal Vehicle Speed Estimation for Four-Wheel-Independently-Actuated Electric Vehicles Based on Multi-Sensor Fusion. *IEEE Trans. Veh. Technol.* **2020**, *69*, 12797–12806. [CrossRef]
- Zhang, L.; Wang, Y.; Wang, Z. Robust Lateral Motion Control for In-Wheel-Motor-Drive Electric Vehicles with Network Induced Delays. *IEEE Trans. Veh. Technol.* **2019**, *68*, 10585–10593. [CrossRef]
- Hannan, M.A.; Lipu, M.S.H.; Ker, P.J.; Begum, R.A.; Agelidis, V.G.; Blaabjerg, F. Power electronics contribution to renewable energy conversion addressing emission reduction: Applications, issues, and recommendations. *Appl. Energy* **2019**, *251*, 113404. [CrossRef]
- Miri, I.; Fotouhi, A.; Ewin, N. Electric vehicle energy consumption modelling and estimation—A case study. *Int. J. Energy Res.* **2020**, 5700. [CrossRef]

17. Javorski Eckert, J.; Corrêa de Alkmin e Silva, L.; Mazzariol Santicioli, F.; dos Santos Costa, E.; Corrêa, F.C.; Giuseppe Dedini, F. Energy storage and control optimization for an electric vehicle. *Int. J. Energy Res.* **2018**, *42*, 3506–3523. [[CrossRef](#)]
18. Wu, J.; Wu, Z.; Wu, F.; Mao, X. A power balancing method of distributed generation and electric vehicle charging for minimizing operation cost of distribution systems with uncertainties. *Energy Sci. Eng.* **2017**, *5*, 167–179. [[CrossRef](#)]
19. Manzetti, S.; Mariasiu, F. Electric vehicle battery technologies: From present state to future systems. *Renew. Sustain. Energy Rev.* **2015**, *51*, 1004–1012. [[CrossRef](#)]
20. Pollet, B.G.; Staffell, I.; Shang, J.L. Current status of hybrid, battery and fuel cell electric vehicles: From electrochemistry to market prospects. *Electrochim. Acta* **2012**, *84*, 235–249. [[CrossRef](#)]
21. Moura, S.J.; Fathy, H.K.; Callaway, D.S.; Stein, J.L. A stochastic optimal control approach for power management in plug-in hybrid electric vehicles. *IEEE Trans. Control. Syst. Technol.* **2011**, *19*, 545–555. [[CrossRef](#)]
22. Zhai, L.; Hu, G.; Lv, M.; Zhang, T.; Hou, R. Comparison of Two Design Methods of EMI Filter for High Voltage Power Supply in DC-DC Converter of Electric Vehicle. *IEEE Access* **2020**, *8*, 66564–66577. [[CrossRef](#)]
23. Gomez Navarro, F.J.; Yebra, L.J.; Gomez Medina, F.J.; Gimenez-Fernandez, A. DC-DC Linearized Converter Model for Faster Simulation of Lightweight Urban Electric Vehicles. *IEEE Access* **2020**, *8*, 85380–85394. [[CrossRef](#)]
24. Elsayad, N.; Moradisizkoochi, H.; Mohammed, O.A. A New Hybrid Structure of a Bidirectional DC-DC Converter with High Conversion Ratios for Electric Vehicles. *IEEE Trans. Veh. Technol.* **2020**, *69*, 194–206. [[CrossRef](#)]
25. Zhang, L.; Hu, X.; Wang, Z.; Ruan, J.; Ma, C.; Song, Z.; Dorrell, D.G.; Pecht, M.G. Hybrid electrochemical energy storage systems: An overview for smart grid and electrified vehicle applications. *Renew. Sustain. Energy Rev.* **2020**, 110581. [[CrossRef](#)]
26. Lai, C.M.; Cheng, Y.H.; Hsieh, M.H.; Lin, Y.C. Development of a Bidirectional DC/DC Converter with Dual-Battery Energy Storage for Hybrid Electric Vehicle System. *IEEE Trans. Veh. Technol.* **2018**, *67*, 1036–1052. [[CrossRef](#)]
27. Kanamarlapudi, V.R.K.; Wang, B.; Kandasamy, N.K.; So, P.L. A New ZVS Full-Bridge DC-DC Converter for Battery Charging with Reduced Losses Over Full-Load Range. *IEEE Trans. Ind. Appl.* **2018**, *54*, 571–579. [[CrossRef](#)]
28. Fardahar, S.M.; Sabahi, M. New Expandable Switched-Capacitor/Switched-Inductor High-Voltage Conversion Ratio Bidirectional DC-DC Converter. *IEEE Trans. Power Electron.* **2020**, *35*, 2480–2487. [[CrossRef](#)]
29. Sayed, K. Zero-voltage soft-switching DC-DC converterbased charger for LV battery in hybrid electric vehicles. *IET Power Electron.* **2019**, *12*, 3389–3396. [[CrossRef](#)]
30. Moradisizkoochi, H.; Elsayad, N.; Mohammed, O.A. Experimental Verification of a Double-Input Soft-Switched DC-DC Converter for Fuel Cell Electric Vehicle with Hybrid Energy Storage System. *IEEE Trans. Ind. Appl.* **2019**, *55*, 6451–6465. [[CrossRef](#)]
31. Lei, J.; Zhou, B.; Wei, J.; Bian, J.; Zhu, Y.; Yu, J.; Yang, Y. Predictive Power Control of Matrix Converter with Active Damping Function. *IEEE Trans. Ind. Electron.* **2016**, *63*, 4550–4559. [[CrossRef](#)]
32. Thirumalaivasan, R.; Xu, Y.; Janaki, M. Power control with z-source converter based unified power flow controller. *IEEE Trans. Power Electron.* **2017**, *32*, 9413–9423. [[CrossRef](#)]
33. Pedroso, M.D.; Nascimento, C.B.; Tusset, A.M.; Kaster, M.D.S. Performance comparison between nonlinear and linear controllers with weighted adaptive control applied to a buck converter using poles placement design. In Proceedings of the International Symposium on Industrial Electronics, Taiwan, China, 28–31 May 2013; Institute of Electrical and Electronics Engineers Inc.: New York, NY, USA; pp. 1–6.
34. Bhat, V.S.; Kumar, V.; Dayanand, N.; Shettigar, A.; Nikhitha. Comparative study of PID control algorithms for an electric vehicle. In Proceedings of the AIP Conference Proceedings, Jaipur, India, 5–6 March 2020; American Institute of Physics Inc.: College Park, MD, USA, 2020; Volume 2236, p. 80001.
35. Babaei, F.; Lashkari, Z.B.; Safari, A.; Farrokhifar, M.; Salehi, J. Salp swarm algorithm-based fractional-order PID controller for LFC systems in the presence of delayed EV aggregators. *IET Electr. Syst. Transp.* **2020**, *10*, 259–267. [[CrossRef](#)]
36. Hannan, M.A.; Ali, J.A.; Ker, P.J.; Mohamed, A.; Lipu, M.S.H.; Hussain, A. Switching Techniques and Intelligent Controllers for Induction Motor Drive: Issues and Recommendations. *IEEE Access* **2018**, *6*, 47489–47510. [[CrossRef](#)]
37. Hannan, M.A.; Islam, N.N.; Mohamed, A.; Lipu, M.S.H.; Ker, P.J.; Rashid, M.M.; Shareef, H. Artificial Intelligent Based Damping Controller Optimization for the Multi-Machine Power System: A Review. *IEEE Access* **2018**, *6*, 39574–39594. [[CrossRef](#)]
38. Parra, A.; Zubizarreta, A.; Pérez, J.; Dendaluze, M. Intelligent Torque Vectoring Approach for Electric Vehicles with Per-Wheel Motors. *Complexity* **2018**, *2018*, 1–15. [[CrossRef](#)]
39. Hassan, S.; Kamal, T.; Riaz, M.; Shah, S.; Ali, H.; Riaz, M.; Sarmad, M.; Zahoor, A.; Khan, M.; Miqueleiz, J. Intelligent Control of Wind-Assisted PHEVs Smart Charging Station. *Energies* **2019**, *12*, 909. [[CrossRef](#)]
40. Pérez-Pimentel, Y.; Osuna-Galán, I.; Avilés-Cruz, C.; Villegas-Cortez, J. Power supply management for an electric vehicle using fuzzy logic. *Appl. Comput. Intell. Soft Comput.* **2018**, *2018*, 1–9. [[CrossRef](#)]
41. Yao, E.; Liu, T.; Lu, T.; Yang, Y. Optimization of electric vehicle scheduling with multiple vehicle types in public transport. *Sustain. Cities Soc.* **2020**, *52*, 101862. [[CrossRef](#)]
42. Shen, Z.J.M.; Feng, B.; Mao, C.; Ran, L. Optimization models for electric vehicle service operations: A literature review. *Transp. Res. Part. B Methodol.* **2019**, *128*, 462–477. [[CrossRef](#)]
43. Nguyen, D.-D.; Bui, N.-T.; Yukita, K. Design and optimization of three-phase dual-active-bridge converters for electric vehicle charging stations. *Energies* **2020**, *13*, 150. [[CrossRef](#)]
44. Aymen, F.; Mahmoudi, C. A novel energy optimization approach for electrical vehicles in a smart city. *Energies* **2019**, *12*, 929. [[CrossRef](#)]

45. Chakraborty, S.; Vu, H.-N.; Hasan, M.M.; Tran, D.-D.; Baghdadi, M.E.; Hegazy, O. DC-DC Converter Topologies for Electric Vehicles, Plug-in Hybrid Electric Vehicles and Fast Charging Stations: State of the Art and Future Trends. *Energies* **2019**, *12*, 1569. [[CrossRef](#)]
46. Jagadeesh, I.; Indragandhi, V. Review and comparative analysis on dc-dc converters used in electric vehicle applications. In Proceedings of the IOP Conference Series: Materials Science and Engineering, Bangkok, Thailand, 17–19 May 2019; Institute of Physics Publishing: Bristol, UK, 2019; Volume 623, p. 12005.
47. Bellur, D.M.; Kazimierczuk, M.K. DC-DC converters for electric vehicle applications. In Proceedings of the 2007 Electrical Insulation Conference and Electrical Manufacturing Expo, Nashville, TN, USA, 22–24 October 2007; pp. 286–293.
48. Anbazhagan, L.; Ramiah, J.; Krishnaswamy, V.; Jayachandran, D.N. A comprehensive Review on Bidirectional Traction Converter for Electric Vehicles. *Int. J. Electron. Telecommun.* **2019**, *65*, 635–649. [[CrossRef](#)]
49. Krithika, V.; Subramani, C. A comprehensive review on choice of hybrid vehicles and power converters, control strategies for hybrid electric vehicles. *Int. J. Energy Res.* **2018**, *42*, 1789–1812. [[CrossRef](#)]
50. Kumar, D.; Nema, R.K.; Gupta, S. A comparative review on power conversion topologies and energy storage system for electric vehicles. *Int. J. Energy Res.* **2020**, *44*, 7863–7885. [[CrossRef](#)]
51. Lipu, M.S.H.; Hannan, M.A.; Hussain, A.; Saad, M.H.M.; Ayob, A.; Uddin, M. Extreme Learning Machine Model for State of Charge Estimation of Lithium-ion battery Using Gravitational Search Algorithm. *IEEE Trans. Ind. Appl.* **2019**, *55*, 4225–4234. [[CrossRef](#)]
52. Liu, Y.; Huang, Z.; Liao, H.; Lyu, C.; Zhou, Y.; Jiao, Y.; Li, H.; Hu, C.; Peng, J. A Temperature-Suppression Charging Strategy for Supercapacitor Stack with Lifetime Maximization. *IEEE Trans. Ind. Appl.* **2019**, *55*, 6173–6183. [[CrossRef](#)]
53. Mukherjee, N.; Strickland, D. Control of Cascaded DC-DC Converter-Based Hybrid Battery Energy Storage Systems-Part I: Stability Issue. *IEEE Trans. Ind. Electron.* **2016**, *63*, 2340–2349. [[CrossRef](#)]
54. Wang, Y.X.; Yu, D.H.; Chen, S.A.; Kim, Y.B. Robust DC/DC converter control for polymer electrolyte membrane fuel cell application. *J. Power Sources* **2014**, *261*, 292–305. [[CrossRef](#)]
55. Ma, X.; Wang, P.; Bi, H.; Wang, Z. A Bidirectional LLCL Resonant DC-DC Converter with Reduced Resonant Tank Currents and Reduced Voltage Stress of the Resonant Capacitor. *IEEE Access* **2020**, *8*, 125549–125564. [[CrossRef](#)]
56. Fardoun, A.A.; Ismail, E.H.; Sabzali, A.J.; Al-Saffar, M.A. Bidirectional converter for high-efficiency fuel cell powertrain. *J. Power Sources* **2014**, *249*, 470–482. [[CrossRef](#)]
57. Dotelli, G.; Ferrero, R.; Gallo Stampino, P.; Latorrata, S.; Toscani, S. Supercapacitor Sizing for Fast Power Dips in a Hybrid Supercapacitor-PEM Fuel Cell System. *IEEE Trans. Instrum. Meas.* **2016**, *65*, 2196–2203. [[CrossRef](#)]
58. Kasichyanula, S.; John, V. Adaptive Control Strategy for Ultracapacitor Based Bidirectional DC-DC Converters. *IEEE Trans. Ind. Appl.* **2019**, *55*, 1717–1728. [[CrossRef](#)]
59. Gorji, S.A.; Sahebi, H.G.; Ektesabi, M.; Rad, A.B. Topologies and control schemes of bidirectional DC-DC power converters: An overview. *IEEE Access* **2019**, *7*, 117997–118019. [[CrossRef](#)]
60. Maroti, P.K.; Padmanaban, S.; Blaabjerg, F.; Fedák, V.; Siano, P.; Ramachandaramurthy, V.K. A novel switched inductor configuration for modified SEPIC DC-to-DC converter for renewable energy application. In Proceedings of the IEEE Conference on Energy Conversion, Kuala Lumpur, Malaysia, 30–31 October 2017; Institute of Electrical and Electronics Engineers Inc.: New York, NY, USA, 2017; pp. 218–223.
61. Liu, H.; Dahidah, M.S.A.; Yu, J.; Naayagi, R.T.; Armstrong, M. Design and Control of Unidirectional DC-DC Modular Multilevel Converter for Offshore DC Collection Point: Theoretical Analysis and Experimental Validation. *IEEE Trans. Power Electron.* **2019**, *34*, 5191–5208. [[CrossRef](#)]
62. Zahid, Z.U.; Dalala, Z.M.; Chen, R.; Chen, B.; Lai, J.S. Design of bidirectional DC-DC resonant converter for Vehicle-to-Grid (V2G) applications. *IEEE Trans. Transp. Electrification* **2015**, *1*, 232–244. [[CrossRef](#)]
63. Ananthapadmanabha, B.R.; Maurya, R.; Arya, S.R. Improved Power Quality Switched Inductor Cuk Converter for Battery Charging Applications. *IEEE Trans. Power Electron.* **2018**, *33*, 9412–9423. [[CrossRef](#)]
64. Shaneh, M.; Adib, E.; Niroomand, M. An Ultrahigh Step-Up Nonisolated Interleaved Converter with Low Input Current Ripple. *IEEE J. Emerg. Sel. Top. Power Electron.* **2020**, *8*, 1584–1592. [[CrossRef](#)]
65. Hu, X.; Ma, P.; Wang, J.; Tan, G. A Hybrid Cascaded DC-DC Boost Converter with Ripple Reduction and Large Conversion Ratio. *IEEE J. Emerg. Sel. Top. Power Electron.* **2020**, *8*, 761–770. [[CrossRef](#)]
66. Ardi, H.; Ajami, A. Study on a High Voltage Gain SEPIC-Based DC-DC Converter with Continuous Input Current for Sustainable Energy Applications. *IEEE Trans. Power Electron.* **2018**, *33*, 10403–10409. [[CrossRef](#)]
67. Azizkandi, M.E.; Sedaghati, F.; Shayeghi, H.; Blaabjerg, F. A High Voltage Gain DC-DC Converter Based on Three Winding Coupled Inductor and Voltage Multiplier Cell. *IEEE Trans. Power Electron.* **2020**, *35*, 4558–4567. [[CrossRef](#)]
68. Shreelakshmi, M.P.; Das, M.; Agarwal, V. Design and Development of a Novel High Voltage Gain, High-Efficiency Bidirectional DC-DC Converter for Storage Interface. *IEEE Trans. Ind. Electron.* **2019**, *66*, 4490–4501. [[CrossRef](#)]
69. Li, W.; Jiang, Q.; Mei, Y.; Li, C.; Deng, Y.; He, X. Modular multilevel DC/DC converters with phase-shift control scheme for high-voltage DC-based systems. *IEEE Trans. Power Electron.* **2015**, *30*, 99–107. [[CrossRef](#)]
70. Jin, K.; Liu, C. A Novel PWM High Voltage Conversion Ratio Bidirectional Three-Phase DC/DC Converter with Y- $\Delta$  Connected Transformer. *IEEE Trans. Power Electron.* **2016**, *31*, 81–88. [[CrossRef](#)]

71. Bandeira, D.G.; Lazzarin, T.B.; Barbi, I. High Voltage Power Supply Using a T-Type Parallel Resonant DC-DC Converter. *IEEE Trans. Ind. Appl.* **2018**, *54*, 2459–2470. [[CrossRef](#)]
72. Turksoy, A.; Teke, A.; Alkaya, A. A comprehensive overview of the dc-dc converter-based battery charge balancing methods in electric vehicles. *Renew. Sustain. Energy Rev.* **2020**, *133*, 110274. [[CrossRef](#)]
73. Affam, A.; Buswig, Y.M.; Othman, A.K.B.H.; Julai, N.B.; Qays, O. A review of multiple input DC-DC converter topologies linked with hybrid electric vehicles and renewable energy systems. *Renew. Sustain. Energy Rev.* **2021**, *135*, 110186. [[CrossRef](#)]
74. Hossain, M.Z.; Rahim, N.A.; Selvaraj, J. a/l Recent progress and development on power DC-DC converter topology, control, design and applications: A review. *Renew. Sustain. Energy Rev.* **2018**, *81*, 205–230. [[CrossRef](#)]
75. Sivakumar, S.; Sathik, M.J.; Manoj, P.S.; Sundararajan, G. An assessment on performance of DC-DC converters for renewable energy applications. *Renew. Sustain. Energy Rev.* **2016**, *58*, 1475–1485. [[CrossRef](#)]
76. Ahmed, O.A.; Bleijs, J.A.M. An overview of DC-DC converter topologies for fuel cell-ultracapacitor hybrid distribution system. *Renew. Sustain. Energy Rev.* **2015**, *42*, 609–626. [[CrossRef](#)]
77. Zhang, N.; Sutanto, D.; Muttaqi, K.M. A review of topologies of three-port DC-DC converters for the integration of renewable energy and energy storage system. *Renew. Sustain. Energy Rev.* **2016**, *56*, 388–401. [[CrossRef](#)]
78. Kolli, A.; Gaillard, A.; De Bernardinis, A.; Bethoux, O.; Hissel, D.; Khatir, Z. A review on DC/DC converter architectures for power fuel cell applications. *Energy Convers. Manag.* **2015**, *105*, 716–730. [[CrossRef](#)]
79. Rehman, Z.; Al-Bahadly, I.; Mukhopadhyay, S. Multiinput DC-DC converters in renewable energy applications—An overview. *Renew. Sustain. Energy Rev.* **2015**, *41*, 521–539. [[CrossRef](#)]
80. Shoja-Majidabad, S.; Hajizadeh, A. Decentralized adaptive neural network control of cascaded DC-DC converters with high voltage conversion ratio. *Appl. Soft Comput. J.* **2020**, *86*, 105878. [[CrossRef](#)]
81. Sun, K.; Li, K.J.; Wang, M.; Tian, G.; Wang, Z.-d.; Liu, Z. Coordination control for multi-voltage-level dc grid based on the dc-dc converters. *Electr. Power Syst. Res.* **2020**, *178*, 106050. [[CrossRef](#)]
82. Hausberger, T.; Kugi, A.; Eder, A.; Kemmetmüller, W. High-speed nonlinear model predictive control of an interleaved switching DC/DC-converter. *Control. Eng. Pract.* **2020**, *103*, 104576. [[CrossRef](#)]
83. Tran, D.; Chakraborty, S.; Lan, Y.; Van Mierlo, J.; Hegazy, O. Optimized multiport DC/DC converter for vehicle drivetrains: Topology and design optimization. *Appl. Sci.* **2018**, *8*, 1351. [[CrossRef](#)]
84. Prithivi, K.; Sathyapriya, M. An optimized DC-DC converter for electric vehicle application. *Int. J. Mech. Eng. Technol.* **2017**, *8*, 173–182. [[CrossRef](#)]
85. Zheng, Y.; He, F.; Shen, X.; Jiang, X. Energy control strategy of fuel cell hybrid electric vehicle based on working conditions identification. *Energies* **2020**, *13*, 426. [[CrossRef](#)]
86. Li, W.; He, X. Review of nonisolated high-step-up DC/DC converters in photovoltaic grid-connected applications. *IEEE Trans. Ind. Electron.* **2011**, *58*, 1239–1250. [[CrossRef](#)]
87. Tofoli, F.L.; de Castro Pereira, D.; de Paula, W.J.; de Sousa Oliveira Júnior, D. Survey on non-isolated high-voltage step-up dc-dc topologies based on the boost converter. *IET Power Electron.* **2015**, *8*, 2044–2057. [[CrossRef](#)]
88. Mirzaei, A.; Jusoh, A.; Salam, Z.; Adib, E.; Farzanehfard, H. Analysis and design of a high efficiency bidirectional DC-DC converter for battery and ultracapacitor applications. *Simul. Model. Pract. Theory* **2011**, *19*, 1651–1667. [[CrossRef](#)]
89. Fernão Pires, V.; Romero-Cadaval, E.; Vinnikov, D.; Roasto, I.; Martins, J.F. Power converter interfaces for electrochemical energy storage systems—A review. *Energy Convers. Manag.* **2014**, *86*, 453–475. [[CrossRef](#)]
90. Kushwaha, R.; Singh, B. A Power Quality Improved EV Charger with Bridgeless Cuk Converter. In Proceedings of the IEEE International Conference on Power Electronics, Drives and Energy Systems, Chennai, India, 18–21 December 2018; Institute of Electrical and Electronics Engineers Inc.: New York, NY, USA, 2018; pp. 1–6.
91. Pandey, R.; Singh, B. A Power Factor Corrected LLC Resonant Converter for Electric Vehicle Charger Using Cuk Converter. In Proceedings of the IEEE International Conference on Power Electronics, Drives and Energy Systems, Chennai, India, 18–21 December 2018; Institute of Electrical and Electronics Engineers Inc.: New York, NY, USA, 2018; pp. 1–6.
92. Reshma, M.S.; Alias, M.B.; Nair, H.S.; Jose, P. Cuk Converter Fed Electric Vehicles. *IOSR J. Electr. Electron. Eng.* **2017**, 12–27. [[CrossRef](#)]
93. Zhang, Y.; Zhang, W.; Gao, F.; Gao, S.; Rogers, D.J. A Switched-Capacitor Interleaved Bidirectional Converter with Wide Voltage-Gain Range for Super Capacitors in EVs. *IEEE Trans. Power Electron.* **2020**, *35*, 1536–1547. [[CrossRef](#)]
94. Zhang, Y.; Gao, Y.; Li, J.; Sumner, M. Interleaved Switched-Capacitor Bidirectional DC-DC Converter with Wide Voltage-Gain Range for Energy. *IEEE Trans. Power Electron.* **2018**, *33*, 3852–3869. [[CrossRef](#)]
95. Sato, Y.; Member, S.; Uno, M.; Nagata, H. Nonisolated Multiport Converters Based on Integration of PWM Converter and Phase-Shift-Switched Capacitor Converter. *IEEE Trans. Power Electron.* **2020**, *35*, 455–470. [[CrossRef](#)]
96. Zhang, Y.; Gao, Y.; Zhou, L.; Sumner, M. A Switched-Capacitor Bidirectional DC-DC Converter with Wide Voltage Gain Range for Electric Vehicles with Hybrid Energy Sources. *IEEE Trans. Power Electron.* **2018**, *33*, 9459–9469. [[CrossRef](#)]
97. Janabi, A.; Wang, B. Switched-Capacitor Voltage Boost Converter for Electric and Hybrid Electric Vehicle Drives. *IEEE Trans. Power Electron.* **2020**, *35*, 5615–5624. [[CrossRef](#)]
98. Zhang, Y.; Liu, Q.; Gao, Y.; Li, J.; Sumner, M. Hybrid Switched-Capacitor/Switched-Quasi-Z-Source Bidirectional DC-DC Converter with a Wide Voltage Gain Range for Hybrid Energy Sources EVs. *IEEE Trans. Ind. Electron.* **2019**, *66*, 2680–2690. [[CrossRef](#)]

99. Liu, K.; Yang, Z.; Tang, X.; Cao, W. Automotive Battery Equalizers Based on Joint Switched-Capacitor and Buck-Boost Converters. *IEEE Trans. Veh. Technol.* **2020**, *69*, 12716–12724. [[CrossRef](#)]
100. Shang, Y.; Liu, K.; Cui, N.; Wang, N.; Li, K.; Zhang, C. A Compact Resonant Switched-Capacitor Heater for Lithium-Ion Battery Self-Heating at Low Temperatures. *IEEE Trans. Power Electron.* **2020**, *35*, 7134–7144. [[CrossRef](#)]
101. Farakhor, A.; Abapour, M.; Sabahi, M. Study on the derivation of the continuous input current high-voltage gain DC/DC converters. *IET Power Electron.* **2018**, *11*, 1652–1660. [[CrossRef](#)]
102. Bahrami, H.; Farhangi, S.; Iman-Eini, H.; Adib, E. A New Interleaved Coupled-Inductor Nonisolated Soft-Switching Bidirectional DC-DC Converter with High Voltage Gain Ratio. *IEEE Trans. Ind. Electron.* **2018**, *65*, 5529–5538. [[CrossRef](#)]
103. Kosai, H.; McNeal, S.; Jordan, B.; Scofield, J.; Ray, B.; Turgut, Z. Coupled inductor characterization for a high performance interleaved boost converter. *IEEE Trans. Magn.* **2009**, *45*, 4812–4815. [[CrossRef](#)]
104. Liu, H.; Hu, H.; Wu, H.; Xing, Y.; Batarseh, I. Overview of High-Step-Up Coupled-Inductor Boost Converters. *IEEE J. Emerg. Sel. Top. Power Electron.* **2016**, *4*, 689–704. [[CrossRef](#)]
105. Gonzalez-Castano, C.; Vidal-Idiarte, E.; Calvente, J. Design of a bidirectional DC/DC converter with coupled inductor for an electric vehicle application. In Proceedings of the IEEE International Symposium on Industrial Electronics, Edinburgh, UK, 19–21 June 2017; Institute of Electrical and Electronics Engineers Inc.: New York, NY, USA, 2017; pp. 688–693.
106. Kascak, S. Analysis of Bidirectional Converter with Coupled Inductor for Electric Drive Application. In Proceedings of the International Conference on Mechatronics, Control and Automation Engineering, Bangkok, Thailand, 24–25 July 2016; Atlantis Press: Amsterdam, The Netherlands, 2016; pp. 229–232.
107. Ayachit, A.; Hasan, S.U.; Siwakoti, Y.P.; Abdal-Hak, M.; Kazimierczuk, M.K.; Blaabjerg, F. Coupled-inductor bidirectional DC-DC converter for EV charging applications with wide voltage conversion ratio and low parts count. In Proceedings of the 2019 IEEE Energy Conversion Congress and Exposition, ECCE 2019, Baltimore, MD, USA, 29 September–3 October 2019; Institute of Electrical and Electronics Engineers Inc.: New York, NY, USA, 2019; pp. 1174–1179.
108. Wu, H.; Sun, K.; Chen, L.; Zhu, L.; Xing, Y. High Step-Up/Step-Down Soft-Switching Bidirectional DC-DC Converter with Coupled-Inductor and Voltage Matching Control for Energy Storage Systems. *IEEE Trans. Ind. Electron.* **2016**, *63*, 2892–2903. [[CrossRef](#)]
109. Zhu, X.; Zhang, B. High step-up quasi-Z-source DC–DC converters with single switched capacitor branch. *J. Mod. Power Syst. Clean Energy* **2017**, *5*, 537–547. [[CrossRef](#)]
110. Yuan, J.; Yang, Y.; Blaabjerg, F. A Switched Quasi-Z-Source Inverter with Continuous Input Currents. *Energies* **2020**, *13*, 1390. [[CrossRef](#)]
111. Babaei, E.; Zarbil, M.S.; Asl, E.S. A developed structure for DC-DC Quasi-Z-Source converter with high voltage gain and high reliability. *J. Circuits, Syst. Comput.* **2019**, *28*. [[CrossRef](#)]
112. Zhang, Y.; Liu, Q.; Li, J.; Sumner, M. A Common Ground Switched-Quasi-Z-Source Bidirectional DC–DC Converter with Hybrid Energy Sources. *IEEE Trans. Ind. Electron.* **2018**, *65*, 5188–5200. [[CrossRef](#)]
113. Devarajan, R.; Sivaraman, E. A Novel Bidirectional Quasi Z Source Inverter for Electric Vehicle Applications. *J. Crit. Rev.* **2020**, *7*, 1114–1118. [[CrossRef](#)]
114. Hu, S.; Liang, Z.; Fan, D.; He, X. Hybrid Ultracapacitor-Battery Energy Storage System Based on Quasi-Z-source Topology and Enhanced Frequency Dividing Coordinated Control for EV. *IEEE Trans. Power Electron.* **2016**, *31*, 7598–7610. [[CrossRef](#)]
115. Farhani, S.; N'Diaye, A.; Djerdir, A.; Bacha, F. Design and practical study of three phase interleaved boost converter for fuel cell electric vehicle. *J. Power Sources* **2020**, *479*, 228815. [[CrossRef](#)]
116. Hegazy, O.; Barrero, R.; Van Mierlo, J.; Lataire, P.; Omar, N.; Coosemans, T. An advanced power electronics interface for electric vehicles applications. *IEEE Trans. Power Electron.* **2013**, *28*, 5508–5521. [[CrossRef](#)]
117. Nahavandi, A.; Hagh, M.T.; Sharifian, M.B.B.; Danyali, S. A nonisolated multiinput multioutput DC-DC boost converter for electric vehicle applications. *IEEE Trans. Power Electron.* **2015**, *30*, 1818–1835. [[CrossRef](#)]
118. Wu, H.; Sun, K.; Ding, S.; Xing, Y. Topology derivation of nonisolated three-port DC-DC converters from DIC and DOC. *IEEE Trans. Power Electron.* **2013**, *28*, 3297–3307. [[CrossRef](#)]
119. Wu, H.; Xing, Y.; Xia, Y.; Sun, K. A family of non-isolated three-port converters for stand-alone renewable power system. In Proceedings of the IECON 2011—37th Annual Conference of the IEEE Industrial Electronics Society, Melbourne, VIC, Australia, 7–11 November 2011; Institute of Electrical and Electronics Engineers Inc.: New York, NY, USA, 2011; pp. 1030–1035.
120. Banaei, M.R.; Ardi, H.; Alizadeh, R.; Farakhor, A. Non-isolated multi-input-single-output DC/DC converter for photovoltaic power generation systems. *IET Power Electron.* **2014**, *7*, 2806–2816. [[CrossRef](#)]
121. Hegazy, O.; Van Mierlo, J.; Lataire, P. Analysis, modeling, and implementation of a multidevice interleaved DC/DC converter for fuel cell hybrid electric vehicles. *IEEE Trans. Power Electron.* **2012**, *27*, 4445–4458. [[CrossRef](#)]
122. Shang, Y.; Liu, K.; Cui, N.; Zhang, Q.; Zhang, C. A Sine-Wave Heating Circuit for Automotive Battery Self-Heating at Subzero Temperatures. *IEEE Trans. Ind. Inf.* **2020**, *16*, 3355–3365. [[CrossRef](#)]
123. Jwaid, S.; Al-Chlaihawi, M. Multiport Converter in Electrical Vehicles-A Review. *Int. J. Sci. Res. Publ.* **2016**, *6*, 378–382. [[CrossRef](#)]
124. Matsushita, Y.; Noguchi, T.; Kimura, O.; Sunayama, T. Current-doubler based multiport DC/DC converter with galvanic isolation. In Proceedings of the 12th International Conference on Power Electronics and Drive Systems (PEDS), Honolulu, HI, USA, 12–15 December 2017; Institute of Electrical and Electronics Engineers Inc.: New York, NY, USA, 2017; pp. 962–967.

125. Priya, M.S.; Balasubramanian, R. Analysis of multidevice interleaved boost converter for high power applications. In Proceedings of the International Conference on Circuits, Power and Computing Technologies, Nagercoil, India, 20–21 March 2014.
126. Sobrino-Manzanares, F.; Garrigós, A. An interleaved, FPGA-controlled, multi-phase and multi-switch synchronous boost converter for fuel cell applications. *Int. J. Hydrogen Energy* **2015**, *40*, 12447–12456. [[CrossRef](#)]
127. Garrigós, A.; Sobrino-Manzanares, F. Interleaved multi-phase and multi-switch boost converter for fuel cell applications. *Int. J. Hydrogen Energy* **2015**, *40*, 8419–8432. [[CrossRef](#)]
128. Deshmukh, S.H.; Sheikh, A.; Giri, M.M.; Tutakne, D.D.R. High Input Power Factor High Frequency Push-Pull DC/DC Converter. *IOSR J. Electr. Electron. Eng.* **2016**, *11*, 42–47. [[CrossRef](#)]
129. Wu, Q.; Wang, M.; Zhou, W.; Wang, X.; Wang, Q. One Zero-Voltage-Switching Voltage-Fed Three-Phase Push-Pull DC/DC Converter for Electric Vehicle Applications. In Proceedings of the ITEC 2019—2019 IEEE Transportation Electrification Conference and Expo, Detroit, MI, USA, 19–21 June 2019; Institute of Electrical and Electronics Engineers Inc.: New York, NY, USA, 2019; pp. 1–5.
130. Hendra, A.; Hamada, F.; Yusivar, F. Voltage Control in Push-Pull DC-DC Converter using State Space Averaging PID with Soft-Start for Electric Vehicle Auxiliary System. In Proceedings of the International Conference on Instrumentation, Control, and Automation, Bandung, Indonesia, 31 July–2 August 2019; Institute of Electrical and Electronics Engineers Inc.: New York, NY, USA, 2019; pp. 188–193.
131. Daniel, W. *Hart Introduction to Power Electronics*; Prentice Hall: Upper Saddle River, NJ, USA, 1997.
132. Babauta, J.T.; Kerber, M.; Hsu, L.; Phipps, A.; Chadwick, D.B.; Arias-Thode, Y.M. Scaling up benthic microbial fuel cells using flyback converters. *J. Power Sources* **2018**, *395*, 98–105. [[CrossRef](#)]
133. Rashid, M.H. *Power Electronics Handbook*; Elsevier Inc.: Amsterdam, The Netherlands, 2011; ISBN 9780123820365.
134. Taneri, M.C.; Genc, N.; Mamizadeh, A. Analyzing and Comparing of Variable and Constant Switching Frequency Flyback DC-DC Converter. In Proceedings of the 4th International Conference on Power Electronics and their Applications, ICPEA 2019, Elazig, Turkey, 25–27 September 2019; Institute of Electrical and Electronics Engineers Inc.: New York, NY, USA, 2019; pp. 1–6.
135. Kanthimathi, R.; Kamala, J. Analysis of different flyback Converter topologies. In Proceedings of the 2015 International Conference on Industrial Instrumentation and Control, ICIC 2015, Pune, India, 28–30 May 2015; Institute of Electrical and Electronics Engineers Inc.: New York, NY, USA, 2015; pp. 1248–1252.
136. Shen, K.; Zhao, D.; Zhao, G. An Improved Numerical Model of Flyback Converters Considering Parameter Tolerance for Fuel Cell Electric Vehicles. In Proceedings of the IECON Proceedings (Industrial Electronics Conference), Lisbon, Portugal, 14–17 October 2019; IEEE Computer Society: Washington, DC, USA, 2019; pp. 6371–6375.
137. Tseng, K.C.; Lin, J.T.; Cheng, C.A. An integrated derived boost-flyback converter for fuel cell hybrid electric vehicles. In Proceedings of the 1st International Future Energy Electronics Conference, IFEEC 2013, Tainan, Taiwan, 3–6 November 2013; IEEE Computer Society: Washington, DC, USA, 2013; pp. 283–287.
138. Bhattacharya, T.; Umanand, L.; Giri, V.S.; Mathew, K. Multiphase Bidirectional Flyback Converter Topology for Hybrid Electric Vehicles. *IEEE Trans. Ind. Electron.* **2009**, *56*, 78–84. [[CrossRef](#)]
139. Sangeetha, J.; Santhi Mary Antony, A.; Ramya, D. A boosting multi flyback converter for electric vehicle application. *Res. J. Appl. Sci. Eng. Technol.* **2015**, *10*, 1133–1140. [[CrossRef](#)]
140. Kim, D.-H.; Kim, M.-S.; Hussain Nengroo, S.; Kim, C.-H.; Kim, H.-J. LLC Resonant Converter for LEV (Light Electric Vehicle) Fast Chargers. *Electronics* **2019**, *8*, 362. [[CrossRef](#)]
141. Lee, W.S.; Kim, J.H.; Lee, J.Y.; Lee, I.O. Design of an Isolated DC/DC Topology with High Efficiency of over 97% for EV Fast Chargers. *IEEE Trans. Veh. Technol.* **2019**, *68*, 11725–11737. [[CrossRef](#)]
142. Ahn, S.H.; Gong, J.W.; Jang, S.R.; Ryoo, H.J.; Kim, D.H. Design and implementation of enhanced resonant converter for EV fast charger. *J. Electr. Eng. Technol.* **2014**, *9*, 143–153. [[CrossRef](#)]
143. Moradisizkoochi, H.; Elsayad, N.; Mohammed, O.A. Experimental Demonstration of a Modular, Quasi-Resonant Bidirectional DC-DC Converter Using GaN Switches for Electric Vehicles. *IEEE Trans. Ind. Appl.* **2019**, *55*, 7787–7803. [[CrossRef](#)]
144. Vu, H.N.; Choi, W. A Novel Dual Full-Bridge LLC Resonant Converter for CC and CV Charges of Batteries for Electric Vehicles. *IEEE Trans. Ind. Electron.* **2018**, *65*, 2212–2225. [[CrossRef](#)]
145. Bai, C.; Han, B.; Kwon, B.H.; Kim, M. Highly Efficient Bidirectional Series-Resonant DC/DC Converter over Wide Range of Battery Voltages. *IEEE Trans. Power Electron.* **2020**, *35*, 3636–3650. [[CrossRef](#)]
146. Gautam, D.S.; Musavi, F.; Eberle, W.; Dunford, W.G. A zero-voltage switching full-bridge DC—DC converter with capacitive output filter for plug-in hybrid electric vehicle battery charging. *IEEE Trans. Power Electron.* **2013**, *28*, 5728–5735. [[CrossRef](#)]
147. Lin, F.; Wang, Y.; Wang, Z.; Rong, Y.; Yu, H. The design of electric car DC/DC converter based on the phase-shifted full-bridge ZVS control. *Energy Procedia* **2016**, *88*, 940–944. [[CrossRef](#)]
148. Peng, F.Z.; Li, H.; Su, G.J.; Lawler, J.S. A new ZVS bidirectional DC-DC converter for fuel cell and battery application. *IEEE Trans. Power Electron.* **2004**, *19*, 54–65. [[CrossRef](#)]
149. Cho, J.G.; Back, J.W.; Jeong, C.Y.; Rim, G.H. Novel zero-voltage and zero-current-switching full-bridge pwm converter using a simple auxiliary circuit. *IEEE Trans. Ind. Appl.* **1999**, *35*, 15–20.
150. Jeon, S.J.; Cho, G.H. A zero-voltage and zero-current switching full bridge DC-DC converter with transform isolation. *IEEE Trans. Power Electron.* **2001**, *16*, 573–580. [[CrossRef](#)]

151. Pahlevaninezhad, M.; Das, P.; Drobnik, J.; Jain, P.K.; Bakhshai, A. A novel ZVZCS full-bridge DC/DC converter used for electric vehicles. *IEEE Trans. Power Electron.* **2012**, *27*, 2752–2769. [[CrossRef](#)]
152. Aamir, M.; Mekhilef, S.; Kim, H.J. High-Gain Zero-Voltage Switching Bidirectional Converter with a Reduced Number of Switches. *IEEE Trans. Circuits Syst. II Express Briefs* **2015**, *62*, 816–820. [[CrossRef](#)]
153. Bronstein, S.; Ben-Yaakov, S. Design considerations for achieving ZVS in a half bridge inverter that drives a piezoelectric transformer with no series inductor. In Proceedings of the IEEE Annual Power Electronics Specialists Conference, Cairns, Australia, 23–27 June 2002; IEEE Computer Society: Washington, DC, USA, 2002; pp. 585–590.
154. Bairabathina, S.; Balamurugan, S. Review on non-isolated multi-input step-up converters for grid-independent hybrid electric vehicles. *Int. J. Hydrogen Energy* **2020**, *45*, 21687–21713. [[CrossRef](#)]
155. Zhao, C.; Round, S.D.; Kolar, J.W. An isolated three-port bidirectional dc-dc converter with decoupled power flow management. *IEEE Trans. Power Electron.* **2008**, *23*, 2443–2453. [[CrossRef](#)]
156. Khan, S.A.; Islam, M.R.; Guo, Y.; Zhu, J. A New Isolated Multi-Port Converter with Multi-Directional Power Flow Capabilities for Smart Electric Vehicle Charging Stations. *IEEE Trans. Appl. Supercond.* **2019**, *29*, 1–4. [[CrossRef](#)]
157. Forouzesh, M.; Siwakoti, Y.P.; Gorji, S.A.; Blaabjerg, F.; Lehman, B. Step-Up DC–DC Converters: A Comprehensive Review of Voltage-Boosting Techniques, Topologies, and Applications. *IEEE Trans. Power Electron.* **2017**, *32*, 9143–9178. [[CrossRef](#)]
158. Chakraborty, S.; Hasan, M.M.; Abdur Razzak, M. Transformer-less single-phase grid-tie photovoltaic inverter topologies for residential application with various filter circuits. *Renew. Sustain. Energy Rev.* **2017**, *72*, 1152–1166. [[CrossRef](#)]
159. Khanipah, N.H.A.; Azri, M.; Talib, M.H.N.; Ibrahim, Z.; Rahim, N.A. Interleaved boost converter for fuel cell application with constant voltage technique. In Proceedings of the 2017 IEEE Conference on Energy Conversion, CENCON 2017, Kuala Lumpur, Malaysia, 30–31 October 2017; Institute of Electrical and Electronics Engineers Inc.: New York, NY, USA, 2017; pp. 55–60.
160. Bianchi, F.D.; Domínguez-García, J.L.; Gomis-Bellmunt, O. Control of multi-terminal HVDC networks towards wind power integration: A review. *Renew. Sustain. Energy Rev.* **2016**, *55*, 1055–1068. [[CrossRef](#)]
161. Huang, G.; Yuan, X.; Shi, K.; Wu, X. A BP-PID controller-based multi-model control system for lateral stability of distributed drive electric vehicle. *J. Franklin Inst.* **2019**, *356*, 7290–7311. [[CrossRef](#)]
162. Amjadi, Z.; Williamson, S.S. Power-electronics-based solutions for plug-in hybrid electric vehicle energy storage and management systems. *IEEE Trans. Ind. Electron.* **2010**, *57*, 608–616. [[CrossRef](#)]
163. Kang, H.S.; Kim, S.M.; Bak, Y.; Lee, K.B. A controller design for a stability improvement of an integrated charging system in hybrid electric vehicle. *IFAC* **2019**, *52*, 141–146. [[CrossRef](#)]
164. Modulation, P.; Marsadek, M.; Rahmat, N.A.; Hoon, Y.; Aljanad, A. A three-level universal electric vehicle charger based on voltage-oriented control and pulse-width modulation. *Energies* **2019**, *12*, 2375.
165. Saleeb, H.; Sayed, K.; Kassem, A.; Mostafa, R. Control and analysis of bidirectional interleaved hybrid converter with coupled inductors for electric vehicle applications. *Electr. Eng.* **2020**, *102*, 195–222. [[CrossRef](#)]
166. Saleeb, H.; Sayed, K.; Kassem, A.; Mostafa, R. Power management strategy for battery electric vehicles. *IET Electr. Syst. Transp.* **2019**, *9*, 65–74. [[CrossRef](#)]
167. Ferreira, A.A.; Pomilio, J.A.; Spiazzi, G.; de Araujo Silva, L. Energy management fuzzy logic supervisory for electric vehicle power supplies system. *IEEE Trans. Power Electron.* **2008**, *23*, 107–115. [[CrossRef](#)]
168. Adam, K.B.; Ashari, M. Design of bidirectional converter using fuzzy logic controller to optimize battery performance in Electric Vehicle. In Proceedings of the International Seminar on Intelligent Technology and Its Applications, Surabaya, Indonesia, 20–21 May 2015; Institute of Electrical and Electronics Engineers Inc.: New York, NY, USA, 2015; pp. 201–205.
169. Lakshmi Narayana, R.; Sreeramulu Mahesh, G.; Cheepati, K.R.; Yuvaraj, T. A fuzzy logic based controller for the bidirectional converter in an electric vehicle. *Int. J. Eng. Technol.* **2019**, *9*, 58–62.
170. Reddy, K.J.; Sudhakar, N. ANFIS-MPPT control algorithm for a PEMFC system used in electric vehicle applications. *Int. J. Hydrogen Energy* **2019**, *44*, 15355–15369. [[CrossRef](#)]
171. Hussain, S.; Ali, M.U.; Park, G.; Nengroo, S.H.; Khan, M.A.; Kim, H. A real-time bi-adaptive controller-based energy hybrid electric vehicles. *Energies* **2019**, *12*, 4662. [[CrossRef](#)]
172. Vidhya, S.D.; Balaji, M. Hybrid fuzzy PI controlled multi-input DC/DC converter for electric vehicle application. *J. Control. Meas. Electron. Comput. Commun.* **2020**, *61*, 79–91.
173. Yilmaz, U.; Turksoy, O.; Teke, A. Intelligent control of high energy efficient two-stage battery charger topology for electric vehicles. *Energy* **2019**, *186*, 115825. [[CrossRef](#)]
174. Sai Teja, T.; Yaseen, M.D.; Anilkumar, T. Bidirectional DC to DC converter with ANN controller for hybrid electric vehicle. *Int. J. Innov. Technol. Explor. Eng.* **2019**, *8*, 4446–4453.
175. Wang, B.; Wang, C.; Hu, Q.; Ma, G.; Zhou, J. Adaptive sliding mode control with enhanced optimal reaching law for boost converter based hybrid power sources in electric vehicles. *J. Power Electron.* **2019**, *19*, 549–559.
176. Wu, Y.; Huangfu, Y.; Ma, R.; Ravey, A.; Chrenko, D. A strong robust DC-DC converter of all-digital high-order sliding mode control for fuel cell power applications. *J. Power Sour.* **2019**, *413*, 222–232. [[CrossRef](#)]
177. Drakunov, S.V.; Reyhanoglu, M.; Singh, B. Sliding mode control of DC-DC power converters. *IFAC Proc. Vol.* **2009**, *42*, 237–242. [[CrossRef](#)]

178. Dai, P.; Cauet, S.; Coirault, P. Passivity-based control and Sliding Mode Control of hybrid DC power source applied to Hybrid Electric Vehicles. In *Proceedings of the International Conference on Systems and Control, Algiers, Algeria, 29–31 October 2013*; Institute of Electrical and Electronics Engineers Inc.: New York, NY, USA, 2013; pp. 691–696.
179. Wang, J.; Xu, D.; Zhou, H.; Zhou, T. Adaptive fractional order sliding mode control for Boost converter in the Battery/Supercapacitor HESS. *PLoS ONE* **2018**, *13*, e0196501. [[CrossRef](#)] [[PubMed](#)]
180. Liu, K.; Li, K.; Zhang, C. Constrained generalized predictive control of battery charging process based on a coupled thermoelectric model. *J. Power Sources* **2017**, *347*, 145–158. [[CrossRef](#)]
181. Ouyang, Q.; Wang, Z.; Liu, K.; Xu, G.; Li, Y. Optimal Charging Control for Lithium-Ion Battery Packs: A Distributed Average Tracking Approach. *IEEE Trans. Ind. Inf.* **2020**, *16*, 3430–3438. [[CrossRef](#)]
182. Kummara, V.G.R.; Zeb, K.; Muthusamy, A.; Krishna, T.N.V.; Prabhudeva Kumar, S.V.S.V.; Kim, D.H.; Kim, M.S.; Cho, H.G.; Kim, H.J. A comprehensive review of DC–DC converter topologies and modulation strategies with recent advances in solar photovoltaic systems. *Electronics* **2020**, *9*, 31. [[CrossRef](#)]
183. Prabaharan, N.; Palanisamy, K. A comprehensive review on reduced switch multilevel inverter topologies, modulation techniques and applications. *Renew. Sustain. Energy Rev.* **2017**, *76*, 1248–1282. [[CrossRef](#)]
184. Salehahari, S.; Babaei, E. A new hybrid multilevel inverter based on coupled-inductor and cascaded H-bridge. In *Proceedings of the 2016 13th International Conference on Electrical Engineering/Electronics, Computer, Telecommunications and Information Technology, ECTI-CON 2016, Chiang Mai, Thailand, 28 June–1 July 2016*; Institute of Electrical and Electronics Engineers Inc.: New York, NY, USA, 2016; pp. 1–6.
185. Seeman, M.D.; Sanders, S.R. Analysis and optimization of switched-capacitor DC-DC converters. *IEEE Trans. Power Electron.* **2008**, *23*, 841–851. [[CrossRef](#)]
186. Busquets-Monge, S.; Crebier, J.C.; Ragon, S.; Hertz, E.; Boroyevich, D.; Gürdal, Z.; Arpilliere, M.; Lindner, D.K. Design of a boost power factor correction converter using optimization techniques. *IEEE Trans. Power Electron.* **2004**, *19*, 1388–1396. [[CrossRef](#)]
187. De Leon-Aldaco, S.E.; Calleja, H.; Aguayo Alquicira, J. Metaheuristic Optimization Methods Applied to Power Converters: A Review. *IEEE Trans. Power Electron.* **2015**, *30*, 6791–6803. [[CrossRef](#)]
188. Liu, K.; Zou, C.; Li, K.; Wik, T. Charging pattern optimization for lithium-ion batteries with an electrothermal-aging model. *IEEE Trans. Ind. Inf.* **2018**, *14*, 5463–5474. [[CrossRef](#)]
189. Liu, K.; Hu, X.; Yang, Z.; Xie, Y.; Feng, S. Lithium-ion battery charging management considering economic costs of electrical energy loss and battery degradation. *Energy Convers. Manag.* **2019**, *195*, 167–179. [[CrossRef](#)]